Digital Comprehensive Summaries of Uppsala Dissertations
from the Faculty of Science and Technology 2322

Creep aspects of softwood from the cell-wall level to structures

RHODEL BENGTSSON

ACTA UNIVERSITATIS
UPSALIENSIS
2023

ISSN 1651-6214
ISBN 978-91-513-1931-5
urn:nbn:se:uu:diva-514316

UPPSALA
UNIVERSITET

Dissertation presented at Uppsala University to be publicly examined in Heinz-Otto Kreiss lecture hall, Ångströmlaboratoriet, Lägerhyddsvägen 1, Uppsala, Friday, 1 December 2023 at 13:15 for the degree of Doctor of Philosophy. The examination will be conducted in English. Faculty examiner: Senior Scientist Dr. Falk Wittel (ETH Zurich).

Abstract

Bengtsson, R. 2023. Creep aspects of softwood from the cell-wall level to structures. *Digital Comprehensive Summaries of Uppsala Dissertations from the Faculty of Science and Technology* 2322. 72 pp. Uppsala: Acta Universitatis Upsaliensis. ISBN 978-91-513-1931-5.

This thesis addresses the intricate mechanical behaviour of natural materials, with a particular focus on wood. Despite millennia of use, understanding the mechanical behaviour of wood materials remains challenging due to their complex microstructures. For instance, they exhibit variations in properties among samples, nonlinear behaviour under elevated loads, and are sensitive to alterations in moisture content.

Wood and related natural biobased materials hold immense potential due to their renewability, cost-effectiveness, eco-friendliness, and ease of use in sustainable construction. Wood boasts remarkable stiffness and strength along its primary axis, surpassing many man-made materials in strength-to-weight ratios. However, its anisotropic and heterogeneous nature gives rise to challenges, necessitating the consideration of multiple parameters for accurate characterization to be used in design.

Wood is intrinsically heterogeneous, leading to considerable variations in local stresses and deformations during loading. To address these microstructural effects on macroscopically measurable phenomena, mathematical homogenization methods, established since the 1970s, have found applications in material mechanics, including both fibre composites and wood.

In recent years, there has been a growing focus on the viscoelastic behaviour of composites and timber structures, given their increased long-term use in load-carrying applications. While numerous investigations have explored the relationship between the microstructure of wood and its elastic properties, few studies have explored the connection between microstructure and viscoelastic properties.

The thesis focuses on the static and, more notably, on the time-dependent mechanical properties of wood, bridging the gap from cell-wall creep to structures. It includes experiments and numerical work, culminating in the development of a material model suitable for orthotropic materials like wood. The multiscale model establishes a link between microstructural parameters and macroscopic properties, potentially applicable to various softwood species. Given the lack of shear creep data in the literature, the thesis introduces straightforward methods to characterize shear creep properties, addressing a significant knowledge gap.

Furthermore, the thesis progresses from material-level experiments to higher length scales, demonstrating how the results can be applied to larger wooden structures, such as the tower for a counter-rotating axis tilted turbine. While these results require further validation in the absence of experimental data for wooden wind turbine structures, they offer useful insights into simulating creep behaviour in such applications.

In conclusion, this thesis highlights the multifaceted nature of a natural material like wood, its mechanical challenges, and the promising research avenues for comprehensive understanding and practical use. The outcome provides contributions to the efficient utilization of wood in load-carrying structures and underlines the importance of ongoing research in this field.

Keywords: Creep, Solid Mechanics, Wooden Materials, Linear Viscoelasticity, Experiments

Rhodel Bengtsson, Department of Materials Science and Engineering, Applied Mechanics, Box 35, Uppsala University, SE-751 03 Uppsala, Sweden.

ISSN 1651-6214
ISBN 978-91-513-1931-5
URN urn:nbn:se:uu:diva-514316 (http://urn.kb.se/resolve?urn=urn:nbn:se:uu:diva-514316)

List of papers

This thesis is based on the following papers, which are referred to in the text by their Roman numerals.

I Bengtsson, R., Afshar, R. and Gamstedt, E.K., 2022. *An applicable orthotropic creep model for wood materials and composites*. Wood Science and Technology, 56(6), pp. 1585-1604.

II Bengtsson, R., Mousavi, M., Afshar, R. and Gamstedt, E.K., 2023. *Viscoelastic behavior of softwood based on a multiscale computational homogenization*. Mechanics of Materials, 179, 104586.

III Bengtsson, R., Bergeron, L., Afshar, R., Mousavi, M. and Gamstedt, E.K., 2023. *Evaluating the viscoelastic shear properties of clear wood via off-axis compression testing and digital-image correlation*. Mechanics of Time-Dependent Materials, pp. 1-15.

IV Bengtsson, R., Florisson, S., Afshar, R., Mousavi, M. and Gamstedt, E.K., 2023. *Comparison of measured creep in a wooden beam with finite element predictions based on orthotropic viscoelastic material model*. Submitted for publication.

V Bengtsson, R., Gamstedt, E.K., Florisson, S. and Bernoff, H., 2023. *Feasiblity of wooden towers for offshore wind turbines: Creep and fatigue predictions*. Submitted for publication.

Reprints were made with permission from the publishers.

Other contributions

The following contributions have been made during the PhD period, but are not included in the thesis

1 Afewerki, S., Wang, X., Ruiz-Esparza, G.U., Tai, C.W., Kong, X., Zhou, S., Welch, K., Huang, P., Bengtsson, R., Xu, C. and Stromme, M., 2020. *Combined catalysis for engineering bioinspired, lignin-based, long-lasting, adhesive, self-mending, antimicrobial hydrogels*. ACS Nano, 14(12), pp.17004-17017.

2 Bengtsson, R., Afshar, R. and Gamstedt, E.K., 2020, October. *A basic orthotropic viscoelastic model for composite and wood materials considering available experimental data and time-dependent Poisson's ratios*. In IOP Conference Series: Materials Science and Engineering (Vol. 942, No. 1, p. 8).

3 Bengtsson, R., Afshar, R,., Mousavi, M. and Gamstedt, E.K., 2022. *Evaluating viscoelastic shear properties in clear wood via off-axis compression testing and digital image correlation*. In Proceedings of the 20th European Conference on Composite Materials - Composites meet sustainability, vol. 6, Vassilopoulos, A. and Michaud, V. (Eds.), EPFL, Lausanne, Switzerland, vol. 1, pp. 270-275..

4 Gamstedt, E.K. and Bengtsson, R., 2022. *Dimensional stability in drying vs. creep in PEG treated waterlogged wooden structures*. In Proceedings of the 15th ICOM-CC Wet Organic Archaeological Materials Working Group Conference, pp. 52-53.

5 Molavitabrizi, D., Bengtsson, R., Botero, C., Rännar, L.E. and Mousavi, S.M., 2022. *Damage-induced failure analysis of additively manufactured lattice materials under uniaxial and multiaxial tension*. International Journal of Solids and Structures, 252, p.111783.

6 Molavitabrizi, D., Khakalo, S., Bengtsson, R., and Mousavi, S.M., 2023. *Second-order homogenization of 3-D lattice materials towards strain gradient media: Numerical modelling and experimental verification*. Continuum Mech. Thermodyn, in press.

Contents

Part I: Introduction 9

1 Motivation 11
1.1 Aims of this thesis 14

Part II: Theoretical Background 17

2 Microscopic features of softwood 19

3 Elastic mechanical properties of wood 20

4 Linear viscoelasticity 22

5 Orthotropic linear viscoelasticity 26
5.1 Finite element implementation 27

6 Computational homogenisation of linear viscoelastic cellular structures 30
6.1 Extraction of the effective properties 31

Part III: Summary of appended papers 33

7 Paper I: Orthotropic linear viscoelasticity 35

8 Paper II: Multiscale model of the linear viscoelastic behaviour of softwoods 39

9 Paper III: Characterization of shear creep using DIC on cubic samples 45

10 Paper IV: Four-point bending creep tests on Norway spruce beam samples 49

11 Paper V: Feasibility of wooden towers for offshore wind turbines: Creep and fatigue predictions 53

Part IV: Conclusions and outlook 57

Summary in Swedish 63

Acknowledgements 65

References 67

Part I:
Introduction

1. Motivation

Natural materials, like wood and other products derived from nature, display intricate mechanical behaviour due to their complex material structures. Despite their millennia-long use [1], it remains challenging to fully grasp their mechanical behaviour. These materials often manifest variations in properties among samples and demonstrate nonlinear behaviour under elevated loads [2, 3, 4]. Alterations in moisture content can lead to significant shrinkage or expansion, further influencing their mechanical attributes [5, 6]. Moreover, these materials, including wood, exhibit loading-rate dependency, manifesting phenomena like creep and viscoelasticity [7].

The potential value of wood and products hailing from natural sources could significantly increase if precise quality assessments of constituent wood and fibres within a log were feasible. These materials hold immense potential due to their cost-effectiveness, eco-friendliness, and renewability [8, 9]. Additionally, their ease of moulding and assembly at construction sites enhances their appeal as preferred construction materials [10].

Wood's structural behaviour embodies both strengths and limitations. It exhibits remarkable stiffness and strength along its primary axis, often surpassing man-made materials in terms of strength-to-weight ratios [11]. Yet, it remains relatively soft and weak in two other directions, potentially predisposing it to cracks and structural failures. Given its anisotropic nature [12], accurately characterizing the mechanical behaviour of wood necessitates accounting for multiple parameters, for example, [13], which could potentially be distilled into key indicators of wood quality.

The variance in mechanical properties of wood originates from diverse natural factors, including distinct growth conditions such as soil type, terrain, and climate variations [14, 15]. Emphasising exhaustive research and comprehension of the mechanical behaviour of wood is pivotal to effectively tackle these challenges. Moreover, harnessing the potential of increasingly robust computer simulation tools for the successful analysis of intricate wood structures requires an in-depth understanding of the physical behaviour of wood materials.

In structures based on wood and wood-plastic composite materials, creep is a major design concern [16, 17, 18]. Mechanical creep is the phenomenon where deformation in a structure increases in time with a constant load. One classic example is bookshelves bending more and more throughout the years

due to the weight of the books. In the creep of most engineering structures, the stress state is generally not uniaxial. Composite and wood-based materials are generally anisotropic, and the deformation behaviour is thus different in different directions. It is often sufficient to assume that these materials are orthotropic to capture the main deformations. Another frequent simplifying assumption is that linear viscoelasticity prevails [19], i.e. the strains are linearly dependent on the stress over time. This assumption has been done multiple times in the context of numerical modelling of viscoelasticity in wood at the macroscale [5, 20, 21, 22]. These aforementioned numerical studies also include mechanosorptive creep, which is creep induced by moisture change in contrast to mechanical creep which is induced by time changes. This type of creep, however, is out of the scope of this thesis as the main assumption in this thesis is that constant climate conditions prevail, as a first step.

However, there are many experimental investigations on the creep properties in the normal directions presented in the works, such as in [13, 23, 24, 25, 26]. On the other hand, there is a striking lack of literature on the shear creep behaviour, of which there are only two papers found in the open literature regarding the characterization of shear creep on wood [27, 28].

Given the highly variable and complex microstructure of wood [29], the creep behaviour also shows a wide variability. The structure of wood is very different at different scales, as is shown in Fig. 1.1. To focus on the most significant features of the microstructure of clear wood, there are three common wood tissues found: the earlywood (EW), the latewood (LW) and the ray cells. The mechanical properties of wood can vary between and within trees from the same species, depending on growth conditions, due to the variability in the relative composition and geometry of the aforementioned tissues. Furthermore, the walls of these cells are made of several layers: S1, S2, S3 and the primary layer, which all could be regarded as fibre laminates in the nano-scale orientated with different microfibril angles (see Fig. 1.1 (f)). As a consequence of the variations of dimensions in the cells, the stiffness between different tree species can be significant. For example, oak can be more than ten times stiffer than balsa [30]. Accurately characterizing the mechanical properties of "wood" can therefore be tricky and, often, requires extensive experimental test campaigns, given the significant variability.

Wood is intrinsically heterogeneous, where the local stresses and deformations may differ considerably during loading. For materials that have repeating elements in their microstructure, homogenization presents itself as a useful method to account for how the microstructural effects macroscopically measurable phenomena. Since the 1970s, mathematical homogenization [31] has found many applications in material mechanics, e.g. for fibre composites and wood [32].

In recent years, more attention has been devoted to the viscoelastic behaviour of composites and timber structures, given the increased long-term use of these materials in load-carrying structures. Although, there have been numerous investigations into the relationship between the microstructure of wood and its elastic properties [33, 34, 35, 36, 37], very few studies regarding the relationship between the microstructure and its viscoelastic properties have been found.

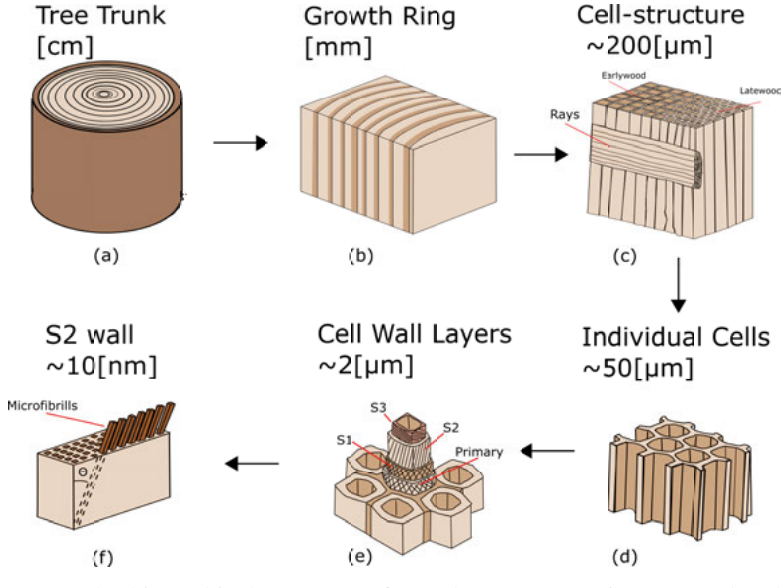

Figure 1.1. The hierarchical structure of wood: (a) A generic tree trunk. (b) The growth rings of wood where the earlywood and latewood tissue alternate. (c) The cell structure is composed of three cell types: earlywood, latewood and ray cells. (d) Generic schematic of a handful of wood cells. (e) The layers of a cell wall. (f) Fibrillar structure of the dominant S2 layers with the microfibril angle θ.

1.1 Aims of this thesis

This thesis aims to investigate and gain insight into the time-dependent mechanical behaviour of wood, see Fig. 1.2. This includes building a model to predict the aforementioned behaviour using homogenization and multiscale modelling techniques. But the thesis also provides new experimental data such as shear creep characterization and 4-point creep bending on Norway spruce which are analyzed using digital image correlation (DIC). The material creep parameters from this study are intended to be used as input for FEM models of various wooden structures that are statically loaded by their self-weight within reasonably extrapolated time frames. The main specific aims of each paper are stated below.

Paper I. The aim was to develop and assess a linear viscoelastic material model able to capture the orthotropic behaviour of wood and fibre materials. The material model is used as the foundation for the subsequent numerical studies of this thesis.

Paper II. The aim was to investigate how the microstructure of softwoods affects their macroscopic elastic and linear viscoelastic behaviour. The study aims to show that the variability in microstructural geometrical parameters has a large influence on the macroscopic properties.

Paper III. From the literature review on the creep behaviour of wood for the previous works, a striking lack of shear creep properties was noticed. The aim was to develop a methodology for the characterization of shear creep parameters of softwood, which in return facilitates the validation of numerical works of creep in wood.

Paper IV. The aim was to further verify the multiscale model developed in Paper II. An experimental 4-point bending creep setup is developed to capture the deflection and strains using DIC in 24 hours, which are later compared with a finite element model.

Paper V. The aim was to demonstrate how the aforementioned material model and parameters could be used on a larger wooden structure. In this study, a vertical wind turbine is modelled with simpler boundary conditions and loads equivalent to common load cases appropriate for turbine towers. In addition, a stress-based fatigue analysis is also performed for a complete mechanical analysis.

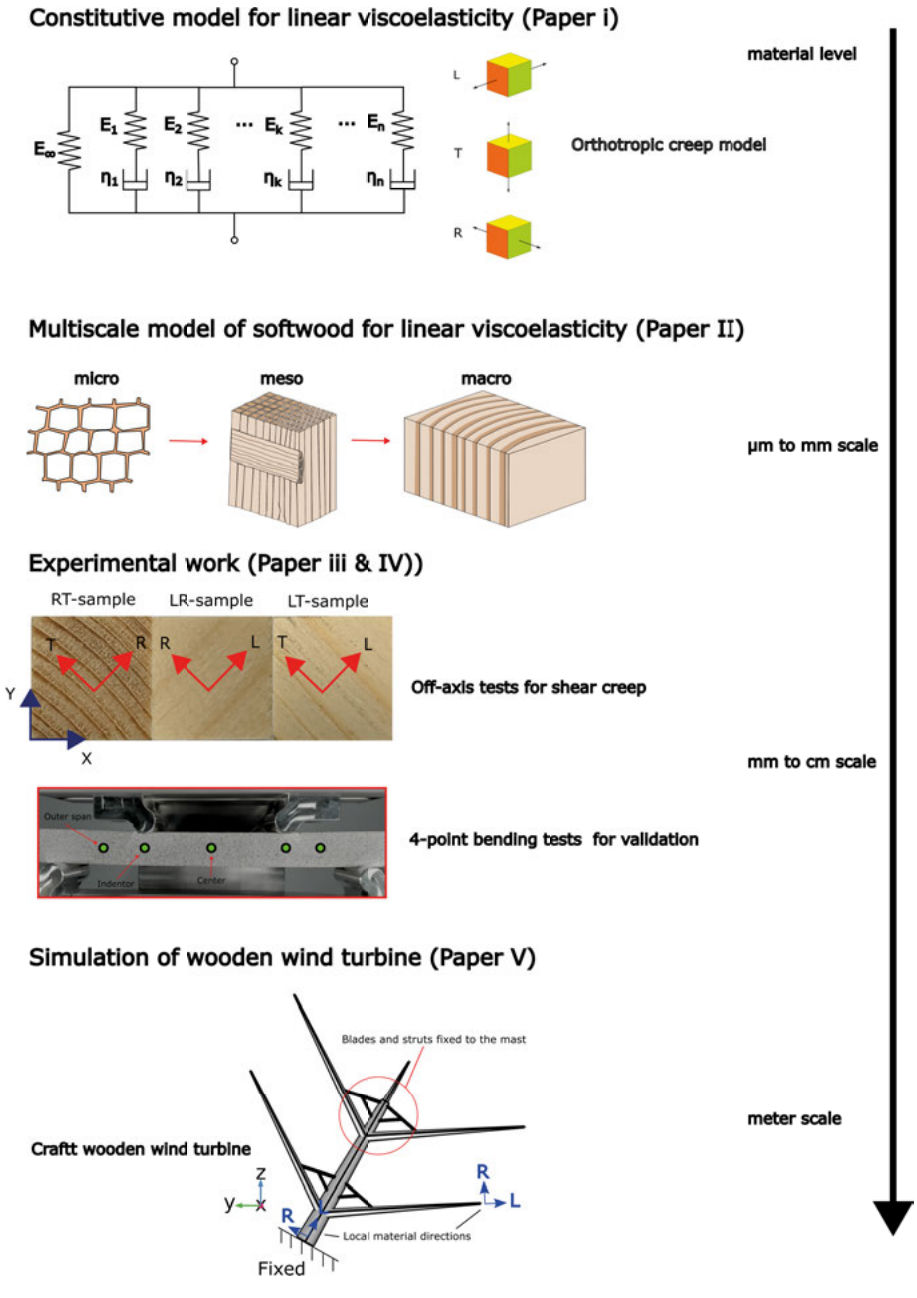

Figure 1.2. Overview of the works in this thesis

Part II:
Theoretical Background

In this part, we explain the theoretical background behind the papers involved in this thesis

2. Microscopic features of softwood

The annual ring of softwood consists primarily of tracheid cells - earlywood (EW), formed during spring, and latewood (LW), formed during summer [38]. Around 90 % of cells in softwoods are these cells and are aligned parallel along the growth direction of the tree [38, 29]. The aforementioned cells provide vertical transportation of fluids and nutrition throughout the tree length but also act as the primary source of structural integrity of the tree. An additional notable feature of wood is the significant presence of ray cells oriented radially from the pith. The orientations and geometry of these are the main cause of the inherent property of anisotropy in wood [12] and therefore is characterized by three main anatomical directions: radial (R), tangential (T), and longitudinal (L). Tracheid cells possess a mean diameter of 30 - 60 μm [29]. Figure 2.1 presents a schematic illustration of wood cell structure, including layers. Depending on their location, cells may possess thin or thick walls. The secondary wall, particularly the S2 layer, confers mechanical stiffness. This layer predominantly consists of microfibrils rich in cellulose, aligned at an angle to the cell's axial direction.

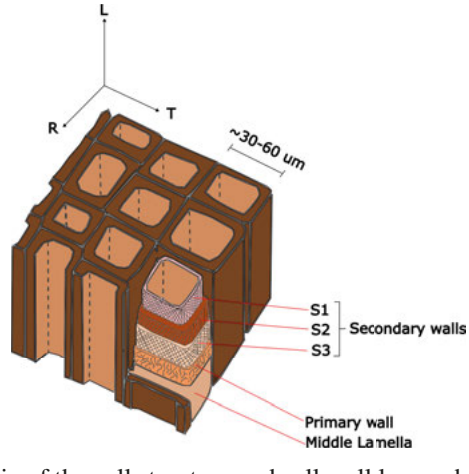

Figure 2.1. Schematic of the cell structure and cell wall layers, based on the depiction of softwood by Ansell [29]

3. Elastic mechanical properties of wood

In general, wood can be characterized as an orthotropic material. This type of material exhibits distinct mechanical properties along three mutually perpendicular axes, which can be aligned with the anatomical axes of a tree. When carefully designing wood structures, it becomes essential to employ a complete set of orthotropic material parameters. This is particularly important for finite element modelling of wood joints that experience localized triaxial stress conditions. For instance, in the FEM modelling of the Vasa ship [39], the decision was made to employ an orthotropic mechanical model for the material.

The stress σ within an elastic material can be determined utilizing Hooke's law, which states that σ within the material is directly proportional to the strains ε. For uniaxial stress, this relationship can be expressed as:

$$\sigma = E\varepsilon \tag{3.1}$$

Here, E represents the elastic constant, commonly known as Young's modulus, measured in Pascals (Pa). Once this constant is determined, it becomes straightforward to compute the strain in the element based on the stress. Wood, as an orthotropic material, exhibits three mutually orthogonal planes of symmetry. If the basis vectors (e_L, e_R, e_T) are normal to these planes of symmetry, then the inverse Hooke's law for wood can be formulated as follows:

$$\begin{bmatrix} \varepsilon_{LL} \\ \varepsilon_{RR} \\ \varepsilon_{TT} \\ \varepsilon_{LR} \\ \varepsilon_{LT} \\ \varepsilon_{RT} \end{bmatrix} = \begin{bmatrix} \frac{1}{E_L} & \frac{-\nu_{LR}}{E_R} & \frac{-\nu_{LT}}{E_T} & 0 & 0 & 0 \\ \frac{-\nu_{RL}}{E_L} & \frac{1}{E_R} & \frac{-\nu_{RT}}{E_T} & 0 & 0 & 0 \\ \frac{-\nu_{TL}}{E_L} & \frac{-\nu_{TR}}{E_R} & \frac{1}{E_T} & 0 & 0 & 0 \\ 0 & 0 & 0 & \frac{1}{G_{LR}} & 0 & 0 \\ 0 & 0 & 0 & 0 & \frac{1}{G_{LT}} & 0 \\ 0 & 0 & 0 & 0 & 0 & \frac{1}{G_{RT}} \end{bmatrix} \begin{bmatrix} \sigma_{LL} \\ \sigma_{RR} \\ \sigma_{TT} \\ \sigma_{LR} \\ \sigma_{LT} \\ \sigma_{RT} \end{bmatrix}. \tag{3.2}$$

Here, G represents the shear moduli, while ν corresponds to the Poisson's ratios. The 6 by 6 matrix shown in equation (3.2) is the compliance matrix denoted as $\boldsymbol{D}$, which serves as the inverse of the stiffness matrix $\boldsymbol{C}$. The cross-diagonal elements of this matrix adhere to the principle of symmetry and can be expressed as follows:

$$\frac{\nu_{TR}}{E_T} = \frac{\nu_{RT}}{E_R}, \quad \frac{\nu_{RL}}{E_R} = \frac{\nu_{LR}}{E_L}, \quad \frac{\nu_{TL}}{E_T} = \frac{\nu_{LT}}{E_L}. \tag{3.3}$$

In the context of a linear elastic orthotropic material, both the stiffness and compliance matrices are composed of nine independent constants, which encompass three for Young's modulus (E), three for shear modulus (G), and three for Poisson's ratio (ν).

4. Linear viscoelasticity

In the following section, an introduction to linear viscoelasticity is given which will be used as the foundation on which new research contribution is built. The readers are referred to the textbooks of Tschoegl [40] and Ottosen and Ristinmaa [41] for a more in-depth description and derivation of linear viscoelasticity. In contrast to linear elastic materials, the behaviour of viscoelastic materials is contingent on their loading history. One common experimental approach for characterizing the linear viscoelastic properties of a material involves conducting a relaxation test. This characterization often takes the form of a uniaxial tensile test with a constant strain ε_0. The stress $\sigma(t)$ is subsequently measured as a function of time, described by the equation:

$$\sigma(t) = \varepsilon_0 E(t). \tag{4.1}$$

Here, $E(t)$ represents the relaxation modulus. In practical applications, there is a need to determine the stress resulting from an arbitrary time-dependent strain history. Consider a prescribed strain in the form of two steps with amplitudes ε_1 and ε_2 occurring at times t_1 and t_2, expressed as:

$$\varepsilon(t) = \varepsilon_1 H(t-t_1) + \varepsilon_2 H(t-t_2), \tag{4.2}$$

where $H(t)$ signifies the Heaviside step function. In the case of linear viscoelastic materials, the stress can be obtained as the sum of responses to these two strain steps:

$$\sigma(t) = \varepsilon_1 E(t-t_1) + \varepsilon_2 E(t-t_2). \tag{4.3}$$

To describe a continuously varying strain history with arbitrary accuracy, it can be approximated as a sum of step functions, as depicted in Figure 4.1. The stress resulting from these individual strain steps, due to linearity, can be formulated as follows:

$$\sigma(t) = \sum_{k=0}^{\infty} \Delta\varepsilon(k\Delta\tau) E(t-k\Delta\tau). \tag{4.4}$$

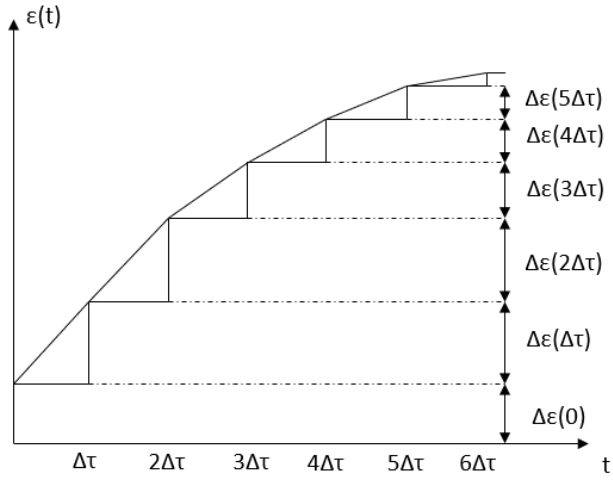

Figure 4.1. Approximation of a continuously varying (and arbitrary) strain history in steps.

By selecting a sufficiently small $\Delta\tau$, a continuously varying stress can be precisely described. For an infinitesimally small $\Delta\tau$, the summation in the above equation can be transformed into an integral:

$$\sigma(t) = \int_{0^-}^{t} E(t-\tau)\frac{d\varepsilon}{d\tau}d\tau, \tag{4.5}$$

This formulation, known as the hereditary approach to linear viscoelasticity, in which linear viscoelasticity is described in integral form when constructing models, in contrast, shows the differential approach that relies on spring-dashpot combinations. The central concept in the hereditary approach is that of superposition.

Creep loading, which is when a constant stress σ_0 is applied on the material, may be treated analogous to the relaxation load case. The strain from a creep test can be described by the creep compliance $J(t)$:

$$\varepsilon(t) = \sigma_0 J(t) \tag{4.6}$$

To retrieve the strains from continuously varying stress history (similar to Fig. 4.1, but with $\sigma(t)$), the same method may be applied when deriving for equation (4.5):

$$\varepsilon(t) = \int_{0^-}^{t} J(t-\tau)\frac{d\sigma}{d\tau}d\tau, \tag{4.7}$$

In this equation, the derivative of potential stress steps is represented by Dirac delta functions. Alternatively, stress steps can be dealt with separately. For a step in stress $\Delta\sigma_0$ at time $t = 0$, the strain is written as follows:

$$\varepsilon(t) = \Delta\sigma_0 J(t) + \int_{0^+}^{t} J(t-\tau)\frac{d\sigma}{d\tau}d\tau, \tag{4.8}$$

Since relaxation modulus and creep compliance are used to describe viscoelasticity, there must be a relationship between these two. According to equation (4.5), if a prescribed strain $\varepsilon(t) = H(t)$ results in a stress $\sigma(t) = E(t)$, then substituting this expression into equation (4.7) yields:

$$H(t) = \int_{0^-}^{t} J(t-\tau)\frac{dE}{d\tau}d\tau, \tag{4.9}$$

Consequently, the relaxation modulus and the creep compliance are interconnected through a convolution integral. If, for example, the relaxation modulus is known, the creep can be determined as a solution to equation (4.9), and vice versa. This relationship can also be derived using the Laplace transform of equations (4.5) and (4.7) with s as the complex frequency:

$$\tilde{\sigma}(s) = s\tilde{E}(s)\tilde{\varepsilon}(s), \quad \tilde{\varepsilon}(s) = s\tilde{J}(s)\tilde{\sigma}(s). \tag{4.10}$$

By eliminating $\tilde{\sigma}(s)$ and $\tilde{\varepsilon}(s)$ from the above equations, a relationship between the Laplace-transformed relaxation $\tilde{E}(s)$ and creep compliance $\tilde{J}(s)$ can be derived:

$$1 = s^2\tilde{E}(s)\tilde{J}(s), \tag{4.11}$$

Which can later be inverse Laplace-transformed into equation (4.9).

An illustration of a frequently used material model that characterizes linear viscoelastic behaviour is the generalized Maxwell model, as depicted in Figure 4.2. To account for arrheodictic behaviour, an additional isolated spring (E_∞) is introduced. A material is considered arrheodictic when it possesses a preferred configuration that prohibits the occurrence of steady-state flow. The response of each Maxwell element, comprising a spring and a dashpot connected in series, is described as follows:

$$\dot{\varepsilon_k} = \frac{\dot{\sigma_k}}{E_k} + \frac{\sigma_k}{\eta_k}, \qquad k = 1,2,3,...n. \tag{4.12}$$

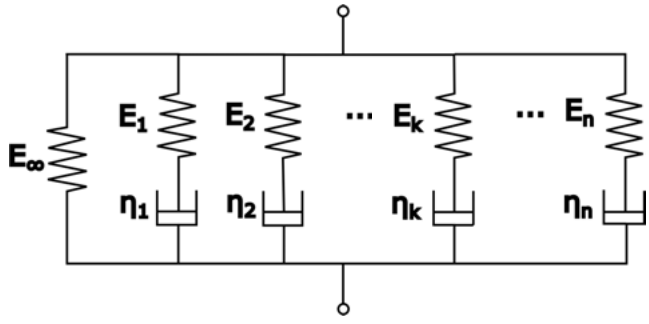

Figure 4.2. A diagram illustrating the generalized Maxwell model comprises n Maxwell elements connected in parallel. Within each Maxwell element, a spring (E_k) and a dashpot (η_k) are connected in series. Additionally, an isolated spring is included in parallel to symbolize the equilibrium modulus (E_∞).

Here, E_k represents the elastic modulus, and η_k represents the viscosity of the kth element. When a constant strain ε_0 is applied at t = 0, the solution to equation (4) is as follows:

$$\sigma_k(t) = \sigma_{k,0} \exp(-t/\tau_k), \qquad \tau_k = \frac{\eta_k}{E_k}, \tag{4.13}$$

where In this context, $\sigma_{k,0}$ represents the initial stress at $t = 0$, and τ_k stands for the relaxation time of the kth element. The overall stress can be expressed as:

$$\sigma(t) = \varepsilon_0 \left[E_\infty + \sum_{k=1}^{n} E_k exp(-t/\tau_k) \right]. \tag{4.14}$$

The relaxation modulus $E(t)$ is defined as

$$E(t) = \sigma(t)/\varepsilon_0 = E_\infty + \sum_{k=1}^{n} E_k exp(-t/\tau_k) \tag{4.15}$$

which essentially represents the Prony series representation. Here, E_∞ signifies the final (or equilibrium) modulus, and $E_0 = E_\infty + \sum_{k=1}^{n} E_k$ is the instantaneous modulus. For any arbitrary strain history, you can insert the above relaxation modulus into equation (4.5). If the material is prescribed by an arbitrary stress history, the relation eq. (4) may be used to transform the relaxation modulus in (4) to an equivalent creep compliance which can be later used in eq. (4.7).

5. Orthotropic linear viscoelasticity

In this section, the orthotropic linear viscoelastic model is presented, which in turn serves as the constitutive model in the numerical implementation of several works in this thesis. Similar works on orthotropic linear viscoelasticity implementations have been done by White and Kim [42] and Zocher [43], but the following derivations have been done specifically for this thesis. In linear viscoelasticity, the stress can be expressed by the convolution integral,

$$\sigma_i(t) = C_{ij}(t)\varepsilon_j(0) + \int_0^t C_{ij}(t-s)\dot{\varepsilon}_j(s)ds \tag{5.1}$$

where s is the variable of integration, σ_i and ε_i are stress and strains in Voigt notation, and C_{ij} are the components of the time-dependent (relaxation) stiffness matrix. Furthermore, C_{ij} is assumed to be described by a Prony series, such that

$$C_{ij}(t) = C_{ij}^{\infty} + \sum_{k=1}^{M} C_{ij}^{(k)} e^{-\frac{t}{\tau_{ij}^{(k)}}}. \tag{5.2}$$

The constants C_{ij}^{∞}, C_{ij}^{k} and τ_{ij}^{k} are the model parameters, and M is the number of terms used in the Prony series. Equation (5.2) is analogous to the 1D Prony series in equation (4). The instantaneous static behaviour can be found inserting (5.2) in (5.1) at $t = 0$:

$$\sigma_i(0) = C_{ij}(0)\varepsilon_j(0) = \left[C_{ij}^{\infty} + \sum_k C_{ij}^{(k)}\right]\varepsilon_j(0), \tag{5.3}$$

The stress at an arbitrary time t can be obtained using a recurrence relation by combining (5.1) and (5.2), resulting in the following expression:

$$\sigma_i(t) = \left[C_{ij}^{\infty} + \sum_k C_{ij}^{(k)} e^{\frac{-t}{\tau_{ij}^{(k)}}}\right]\varepsilon_j(0) + \int_0^t \left[C_{ij}^{\infty} + \sum_k C_{ij}^{(k)} e^{\frac{-t-s}{\tau_{ij}^{(k)}}}\right]\dot{\varepsilon}_j(s)ds, \tag{5.4}$$

which in return can be separated into elastic and viscous parts, namely,

$$\sigma_i(t) = \sigma_{i,\text{elastic}}(t) + \sum_{k=1}^{M} \sigma_{i,\text{viscous}}^{(k)}(t) \tag{5.5}$$

where,

$$\sigma_{i,\text{elastic}} = C_{ij}^{\infty}\left(\varepsilon_j(0) + \int_0^t \dot{\varepsilon}_j(s)ds\right) = C_{ij}^{\infty}\varepsilon_j(t) \tag{5.6}$$

and,

$$\sigma_{i,\text{viscous}}^{(k)} = C_{ij}^{(k)}\left(e^{\frac{-t}{\tau_{ij}^{(k)}}}\varepsilon_j(0) + \int_0^t e^{\frac{-t-s}{\tau_{ij}^{(k)}}}\dot{\varepsilon}_j(s)ds\right). \tag{5.7}$$

In a step-wise integration, it is useful to evaluate the integral in (5.7) by separating it into two domains, $s = [0, t-\Delta t]$ and $s = [t-\Delta t, t]$, resulting in

$$\sigma_{i,\text{viscous}}^{(k)} = C_{ij}^{(k)}\left[e^{\frac{-t}{\tau_{ij}^{(k)}}}\varepsilon_j(0) + \int_0^{t-\Delta t} e^{\frac{-t-s}{\tau_{ij}^{(k)}}}\dot{\varepsilon}_j(s)ds + \int_{t-\Delta t}^{t} e^{\frac{-t-s}{\tau_{ij}^{(k)}}}\dot{\varepsilon}_j(s)ds\right]. \tag{5.8}$$

From (5.7), the viscous stresses are evaluated at time $t-\Delta t$,

$$\begin{aligned}\sigma_{i,\text{viscous}}^{(k)}(t-\Delta t) &= C_{ij}^{(k)}\left[e^{\frac{-t-\Delta t}{\tau_{ij}^{(k)}}}\varepsilon_j(0) + \int_0^{t-\Delta t} e^{\frac{-t-\Delta t-s}{\tau_{ij}^{(k)}}}\dot{\varepsilon}_j(s)ds\right] \\ &= C_{ij}^{k}e^{\frac{-\Delta t}{\tau_{ij}^{(k)}}}\left[e^{\frac{-t}{\tau_{ij}^{(k)}}}\varepsilon_j(0) + \int_0^{t-\Delta t} e^{\frac{-t-s}{\tau_{ij}^{(k)}}}\dot{\varepsilon}_j(s)ds\right].\end{aligned} \tag{5.9}$$

Using eq. (5.9), eq. (5.8) can be rewritten as a recurrence relation

$$\sigma_{i,\text{viscous}}^{(k)} = e^{\frac{-\Delta t}{\tau_{ij}^{(k)}}}\sigma_{i,\text{viscous}}(t-\Delta t) + C_{ij}^{(k)}\int_{t-\Delta t}^{t} e^{\frac{-t-s}{\tau_{ij}^{(k)}}}\dot{\varepsilon}(s)ds \tag{5.10}$$

5.1 Finite element implementation

To implement a material model in finite element software, it is convenient to calculate the stress based on a strain increment and the stress history from the previous time step. This is done by using the relaxation form to derive the viscoelastic constitutive equations. For small time steps Δt, the strain rate $\dot{\varepsilon}_j$ may be considered constant, i.e.

$$\dot{\varepsilon}_j = \frac{\Delta\varepsilon_j}{\Delta t}, \tag{5.11}$$

and (5.10) then transforms into

$$\sigma^{(k)}_{i,\text{viscous}} = e^{\frac{-\Delta t}{\tau^{(k)}_{ij}}} \sigma_{i,\text{viscous}}(t-\Delta t) + \frac{1-e^{\frac{-\Delta t}{\tau^{(k)}_{ij}}}}{\Delta t/\tau^{(k)}_{ij}} C^{(k)}_{ij} \Delta\varepsilon_j. \tag{5.12}$$

From (5.12), it is now possible to obtain the viscous stresses for each time step Δt. It is noted that the viscous stresses at time t are equal to a fraction of the viscous stress from the previous time step plus a stress increment due to the strain increment $\Delta\varepsilon_j$. Finally, the total stress is the sum of the elastic and viscous contributions,

$$\begin{aligned} \sigma_i(t) = C^{\infty}_{ij}\varepsilon_j(t) + \sum_{k=1}^{M} e^{\frac{-\Delta t}{\tau^{(k)}_{ij}}} \sigma_{i,\text{viscous}}(t-\Delta t) \\ + \sum_{k=1}^{M} \frac{1-e^{\frac{-\Delta t}{\tau^{(k)}_{ij}}}}{\Delta t/\tau^{(k)}_{ij}} C^{(k)}_{ij} \Delta\varepsilon_j \end{aligned} \tag{5.13}$$

In addition to the stress update, it is necessary to provide the consistent tangent stiffness, also known as the material Jacobian, to the finite element (FE) software. The consistent tangent stiffness is necessary to derive the constitutive component of the internal virtual work, where the latter is discretized to formulate the FE equations, which are later solved by Newton-Raphson iterations to find the corresponding displacements that yield equilibrium. Differentiating Eq. (5.13) with respect to the strain ε_j, the Jacobian is obtained:

$$C^{\text{tan}}_{ij} = \frac{\partial\sigma_i(t)}{\partial\varepsilon_j(t)} = C^{\infty}_{ij} + \sum_{k=1}^{M} \frac{1-e^{\frac{-\Delta t}{\tau^{(k)}_{ij}}}}{\Delta t/\tau^{(k)}_{ij}} C^{(k)}_{ij}. \tag{5.14}$$

The above formulation may be interchangeably used between different FE software that allows user-written material subroutines. Equation (5.14) may be inserted as "DDSDDE" in Abaqus UMAT, "dsdePL" in Ansys USERMAT or "D" in COMSOL external materials. From Eq. (5.2), it should be noted that this approach will have $9 + 18M$ parameters that need to be defined to model the viscoelasticity of a general 3D orthotropic material. Choosing an adequate number of parameters is often a delicate task. On the other hand, overfitting

by too many empirical parameters does not add any significant predictive precision given the generally large scatter in measured data. The higher-order and less influential parameters could then not be quantified with any meaningful precision.

6. Computational homogenisation of linear viscoelastic cellular structures

The basic idea of homogenisation is to average the behaviour of a material with a complex periodic microstructure by replacing the material with an equivalent homogeneous continuum. With the aid of a homogenisation procedure and the finite element method it is possible to derive the constitutive global behaviour of the corresponding heterogeneous material.

The homogenisation theory will be outlined here for a linear elastic material in which small strains are assumed and geometrical nonlinear effects are neglected. Only basic features of the homogenisation method will be treated in this section. It is assumed that the microstructure of the body is periodic and that the material is composed of subcells of equal shape and material properties. A subcell can then be chosen as a representative volume element that is repeated throughout the body. In the context of this thesis, the RVEs:s are usually the tracheid cells in wood.

Each representative volume element in the body has the same shape and the same material properties with respect to the local coordinate systems. In the undeformed and deformed configurations, adjacent base cells must always fit together at the boundaries. Moreover, for a homogeneous stress field, cells lying far from the boundaries are subjected to the same loading conditions and will deform in the same manner. The possible shapes of the cells in undeformed and deformed configurations are limited in such a way, therefore, that the boundaries of opposing sides of the base cell always have the same shape.

Using the same principles as Yvonnet [44] and Tran et al. [45] to obtain the effective properties of a linear viscoelastic heterogeneous media, we start by defining a localization problem based on strains with no inertial effects. Assuming that a representative volume element (RVE) with domain Ω is subjected to a homogeneous strain field $\bar{\varepsilon} = H(t)\bar{\varepsilon}_{\mathbf{0}}$, where $H(t)$ is the Heaviside step function, we search to find the displacement field $\boldsymbol{u}$ such that

$$\boldsymbol{\nabla} \cdot \boldsymbol{\sigma}(\boldsymbol{u}(\boldsymbol{x})) = 0, \quad \forall \boldsymbol{x} \in \Omega \tag{6.1}$$

using the constitutive description of (5.1), and verify that

$$\langle \boldsymbol{\varepsilon} \rangle = \bar{\varepsilon} \tag{6.2}$$

where

$$\boldsymbol{\varepsilon}(\boldsymbol{u}(\boldsymbol{x})) = \frac{1}{2}(\boldsymbol{\nabla}\boldsymbol{u}(\boldsymbol{x}) + \boldsymbol{\nabla}^T\boldsymbol{u}(\boldsymbol{x})). \tag{6.3}$$

Equations (6.1)-(6.2) may be satisfied and solved for $\boldsymbol{u}$ by applying appropriate boundary conditions. The microscopic strain field $\boldsymbol{\varepsilon}$ is assumed to be the superposition of the applied macroscopic strain $\bar{\boldsymbol{\varepsilon}}$ and a local strain fluctuation $\tilde{\boldsymbol{\varepsilon}}$:

$$\boldsymbol{\varepsilon} = \bar{\boldsymbol{\varepsilon}} + \tilde{\boldsymbol{\varepsilon}} \tag{6.4}$$

Averaging (6.4) yields

$$\langle\boldsymbol{\varepsilon}\rangle = \bar{\boldsymbol{\varepsilon}} + \frac{1}{2V}\int_{\delta\Omega} \tilde{\boldsymbol{u}} \otimes \boldsymbol{n} + \boldsymbol{n} \otimes \tilde{\boldsymbol{u}}\, d\Gamma, \tag{6.5}$$

where V is the volume of the RVE and the fluctuating displacement $\tilde{\boldsymbol{u}}$ is defined as

$$\tilde{\boldsymbol{u}} = \boldsymbol{u} - \bar{\boldsymbol{\varepsilon}}\boldsymbol{x}. \tag{6.6}$$

To satisfy Eq. (6.2), the integral term in Eq. (6.5) has to equal zero. By imposing $\tilde{\boldsymbol{u}}$ as a periodic function on Ω and integrating Eq. (6.4) with respect to $\boldsymbol{x}$, we obtain following boundary condition for our problem,

$$\boldsymbol{u}(\boldsymbol{x}) = \bar{\boldsymbol{\varepsilon}}\boldsymbol{x} + \tilde{\boldsymbol{u}}(\boldsymbol{x}) \quad \forall \boldsymbol{x} \in \delta\Omega, \tag{6.7}$$

which is the periodic boundary condition commonly used in homogenization. Since the fluctuation $\tilde{\boldsymbol{u}}$ takes the same values in two opposite points along the boundary of the RVE, the integral in Eq. (6.5) is equal to zero.

6.1 Extraction of the effective properties

In previous studies [45, 46, 47], it has been shown that if the constituents of a composite are linearly viscoelastic then the overall macroscopic behaviour of the composite is also linearly viscoelastic. Thus, similarly to Eq. (5.1), but in tensorial form, we have

$$\bar{\sigma}_{ij}(t) = \int_0^t \bar{C}_{ijkl}(t-s)\frac{d\bar{\varepsilon}_{kl}}{ds}ds + \bar{C}_{ijkl}(t)\bar{\varepsilon}_{kl}(0) \tag{6.8}$$

where $\bar{\sigma}_{ij}$ and $\bar{\varepsilon}_{kl}$ are the macroscopic stress and strain fields. To determine the effective relaxation tensor $\bar{C}_{ijkl}(t)$ for our RVE, we start by numerically solving for the microscopic stress field σ_{ij} for six different load cases where the average microscopic strain field $\langle\varepsilon\rangle$ is equal to the macroscopic strain field

$\bar{\varepsilon}(t) = H(t)\varepsilon^{kl}$, whereas the components of ε^{kl} are

$$\varepsilon^{(11)} = \begin{pmatrix} 1 & 0 & 0 \\ 0 & 0 & 0 \\ 0 & 0 & 0 \end{pmatrix}; \quad \varepsilon^{(22)} = \begin{pmatrix} 0 & 0 & 0 \\ 0 & 1 & 0 \\ 0 & 0 & 0 \end{pmatrix}; \quad \varepsilon^{(33)} = \begin{pmatrix} 0 & 0 & 0 \\ 0 & 0 & 0 \\ 0 & 0 & 1 \end{pmatrix}$$
$$\varepsilon^{(12)} = \begin{pmatrix} 0 & 0.5 & 0 \\ 0.5 & 0 & 0 \\ 0 & 0 & 0 \end{pmatrix}; \quad \varepsilon^{(13)} = \begin{pmatrix} 0 & 0 & 0.5 \\ 0 & 0 & 0 \\ 0.5 & 0 & 0 \end{pmatrix}; \quad \varepsilon^{(23)} = \begin{pmatrix} 0 & 0 & 0 \\ 0 & 0 & 0.5 \\ 0 & 0.5 & 0 \end{pmatrix}. \tag{6.9}$$

These six different load cases represent different relaxation tests done on our RVE. Using the Hill-Mandel condition,

$$\bar{\boldsymbol{\sigma}} : \bar{\varepsilon} = \langle \boldsymbol{\sigma}(\boldsymbol{x}) : \varepsilon(\boldsymbol{x}) \rangle, \tag{6.10}$$

which prescribes that the macroscopic strain energy is equal to the average strain energy of the RVE along with our constitutive model in the microscopic scale, we obtain the effective relaxation tensor of our RVE:

$$\bar{C}_{ijkl}(t) = \langle \sigma_{ij}(t, \varepsilon^{(kl)}) \rangle, \tag{6.11}$$

where

$$\bar{\sigma}_{ij} = \frac{1}{V} \int_{\Omega} \sigma_{ij} d\Omega = \langle \sigma_{ij}. \rangle \tag{6.12}$$

The macroscopic relaxation tensor $\bar{C}_{ijkl}(t)$ is, however, not known in closed form in the general case. To allow us to develop our multiscale model, we assume instead that $\bar{C}_{ijkl}(t)$ can be described by a Prony series, making it consistent for our FE implementation of the orthotropic linear viscoelastic model outlined in Chapter 5. By sampling the average stress field $\langle \sigma_{ij} \rangle$ at different points of time in the numerical solution, we fit our effective relaxation tensor with a Prony series function, similarly to (5.2).

Part III:
Summary of appended papers

This part is dedicated to examining the appended papers, their key findings, and the subsequent consequences that arise from these studies.

7. Paper I: Orthotropic linear viscoelasticity

In Paper I, an orthotropic linear viscoelastic model is presented and examined in its performance of predicting the time-dependent nature of wood and composites at the material level. The hereditary approach is used to represent the viscoelastic behaviour of orthotropic materials, of which its analytical and finite element derivation is well explained in Section 5. Since constant Poisson's ratios are a common assumption for viscoelastic composites due to lack of data, this study presents the effects of time-dependent Poisson's ratio in the study.

The material model parameters are gained from tuning against creep experiments in which the creep strains in the loading direction as well as transverse direction due to Poisson's effect are captured. A time-dependent creep compliance matrix $\mathbf{D}(t_n)$, in the same form as eq. 3.2, is formulated from the experiments, where all of its component constituents (E, G and ν) are also time-dependent. In this study, the relaxation matrix $\mathbf{C}(t_n)$ is simply found by inverting the newly formulated creep compliance $\mathbf{D}(t_n)$. As $\mathbf{C}(t_n)$ still are just values at discrete times increments from the experiments, they are fitted against the aforementioned Prony series described by eq. (5.2), which is later used as material model parameters for the orthotropic linear viscoelastic formulation. For this study, we also propose cases where we assume constant Poisson's ratios by setting them to their equivalent initial (elastic) values found in the experiments $\nu = \nu(t = 0)$.

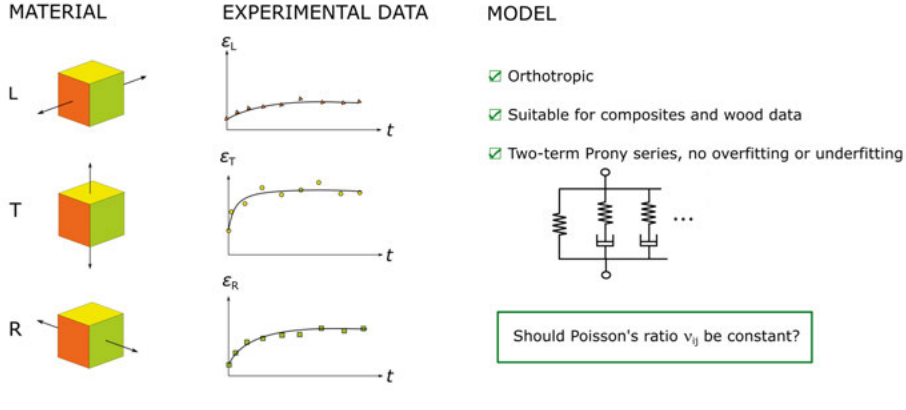

Figure 7.1. Conceptual overview of Paper I, where existing experimental data for orthotropic materials is captured by a balanced rheological model.

With time-dependent Poisson's ratios, the results show that the model can simultaneously capture the time-dependent behaviour in three material axes of orthotropic materials such as European beech wood and a fibre-reinforced composite. However, a relatively poor match was found when the Poisson's ratios were assumed to be constant. Thus, the frequently employed assumption of constant Poisson's ratios should be made with caution.

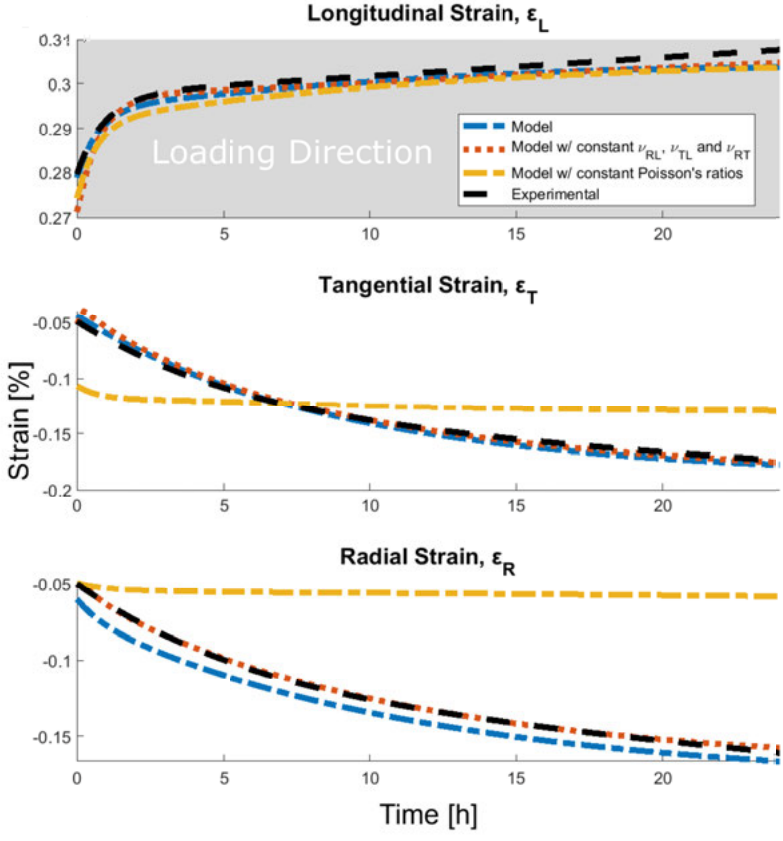

Figure 7.2. Comparison of creep curves between experimental measurement and viscoelastic models with time-dependent and (some) constant Poisson's ratios. Creep curves are presented in the longitudinal, ε_L, tangential direction, ε_T, and radial direction, ε_R, during tensile loading in the longitudinal direction (L). The experimental data for beech wood are from [48].

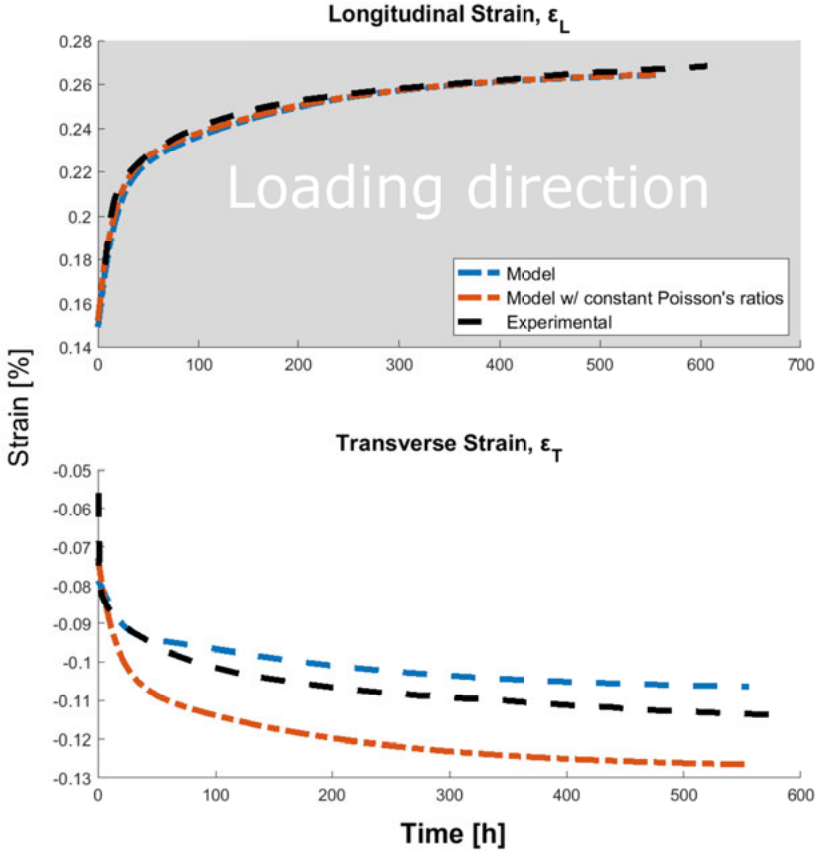

Figure 7.3. Comparison of creep curves between experimental measurement and viscoelastic models with time-dependent and constant Poisson's ratios. Creep curves are presented in the longitudinal, ε_{L}, and transverse direction, ε_{T}, during tensile loading longitudinal direction (L). The experimental data for glass-fibre composite material are from [49].

It has been a common practice in creep analysis to assume that Poisson's ratios remain constant while the elastic moduli change over time. However, this study reveals that keeping Poisson's ratios fixed is generally not recommended unless experimental testing confirms their time independence.

Regarding the method used to extract model parameters from creep tests in this study, there may be a need for re-evaluation. It has been assumed that the inverse of the creep compliance matrix $\mathbf{D}$ corresponds to the relaxation stiffness matrix $\mathbf{C}$. However, analytically, this is not the case, as $\boldsymbol{C}(s)\boldsymbol{D}(s) = 1/s^2$ in the Laplace domain, where 's' represents the complex frequency, as demonstrated in the 1D case (see equation (4)). Nonetheless, it has been practically

shown that taking the matrix inverse in the time domain is sufficient, although this should be done with caution.

In summary, the current approach offers a swift and direct method for developing a creep model based on experimental data, particularly suited for orthotropic materials like wood and composites. This model can be seamlessly incorporated into most finite element software for predicting creep behaviour at the structural or component level.

8. Paper II: Multiscale model of the linear viscoelastic behaviour of softwoods

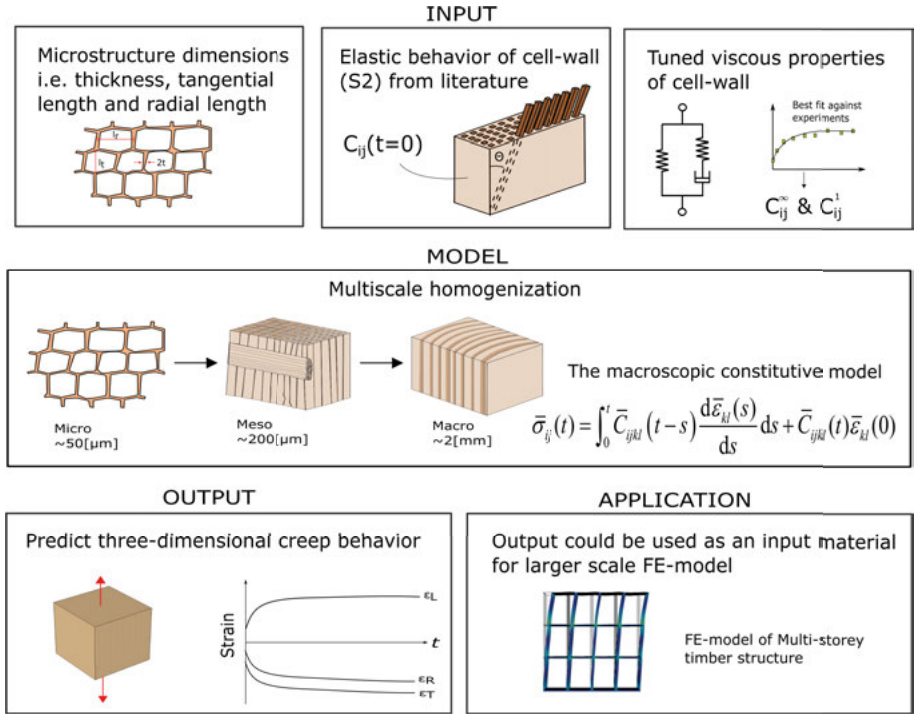

Figure 8.1. Conceptual overview of Paper II: Input requirements are the geometrical dimensions of microstructure, the elastic behaviour of the cell walls (given) as well as the viscous properties (tuned). These input parameters are used in the multiscale model to predict three-dimensional creep. Upscaling to wooden structures is then possible, for different types of wood with inherent microstructural parameters.

To achieve a more realistic viscoelastic modelling of wood, a numerical approach utilizing computational homogenization can be useful. While similar investigations have been conducted on predicting time-dependent behaviour in laminated composites [50, 51], the application of such numerical homogenization techniques to wood has not been extensively explored. In this study, we present a multiscale model of wood based on numerical homogenization, which is compared to experimental data for Norway Spruce and Japanese Cypress. Our approach involves homogenizing the linear viscoelastic properties

of different wood cells, modelled as infinitely long rectangular tubes, and scaling up these properties to the growth ring scale. Unlike the analytical approach [52], numerical homogenization allows for a comprehensive representation in the time domain. This advantage provides greater flexibility in modelling complex structures at different scales and incorporating experimental creep data. By working strictly in the time domain, we avoid potential challenges associated with transforming from the Laplace domain, especially when closed-form solutions for effective properties in the Laplace domain are unavailable. The constitutive model used in this study encompasses orthotropic linear viscoelasticity which was developed and implemented in Paper I, and to the best of my knowledge, it has not been employed in computational homogenization for wood. Although our multiscale model focuses on wood, the approach adopted here is equally applicable to other hierarchical materials such as bamboo [53], which, thus far, have only been subjected to elastic modelling [54].

In Paper II, a numerical multiscale model is presented that explores the influence of the hierarchical structure of softwood on its macroscopic viscoelastic properties. Specifically, the model focuses on two softwood species, Norway spruce and Japanese cypress, which have been experimentally characterized for their creep behaviour. The research findings indicate that by utilizing the same transversely isotropic viscous properties of the cell wall for both species, it is feasible to reasonably predict creep deformation, closely aligning with experimental measurements. The study suggests that the variability in microstructural parameters (such as density, cell-wall geometry, microfibril angle, and composition of wood tissues) outweighs that at the cell-wall level. Therefore, it becomes possible to predict macroscopic creep behaviour solely based on these microstructural parameters. Such predictive capabilities have the potential to save time and costs, as comprehensive creep characterization in all material directions is a demanding task.

The multiscale model is based on tuning the microstructural material parameters against experimental creep test data of softwood species [55, 56] found available in the literature. At each scale, the same material model is implemented which is the linear viscoelastic material model introduced in Section 5. The effective properties of the next scale are retrieved by performing "relaxation" tests as described in Section 6.1.

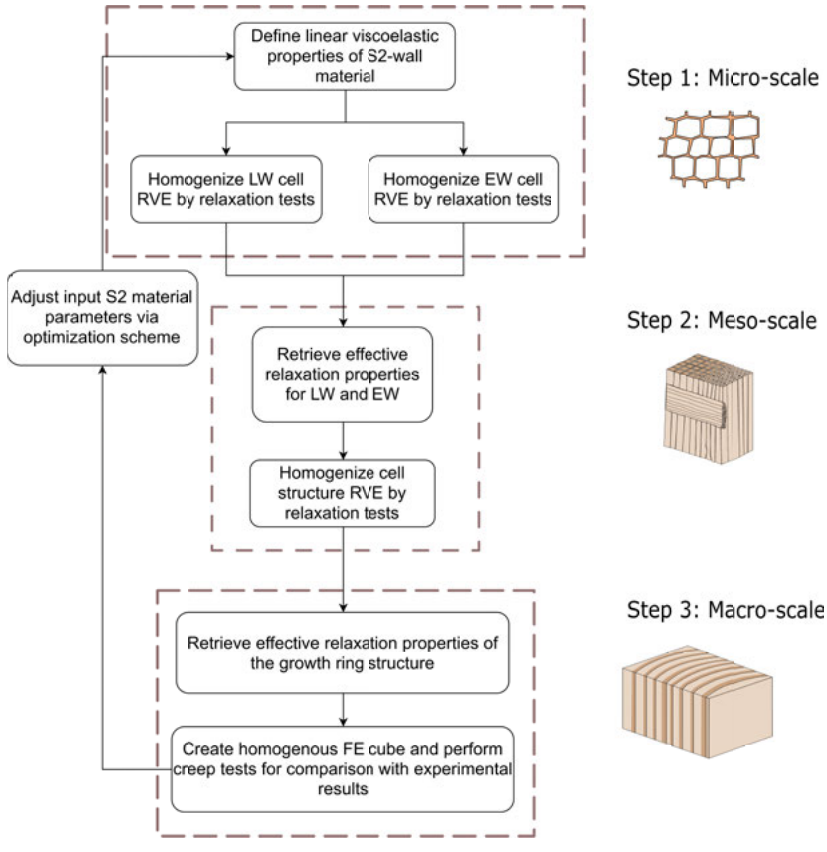

Figure 8.2. Flowchart of the multiscale modelling of softwood in Paper II.

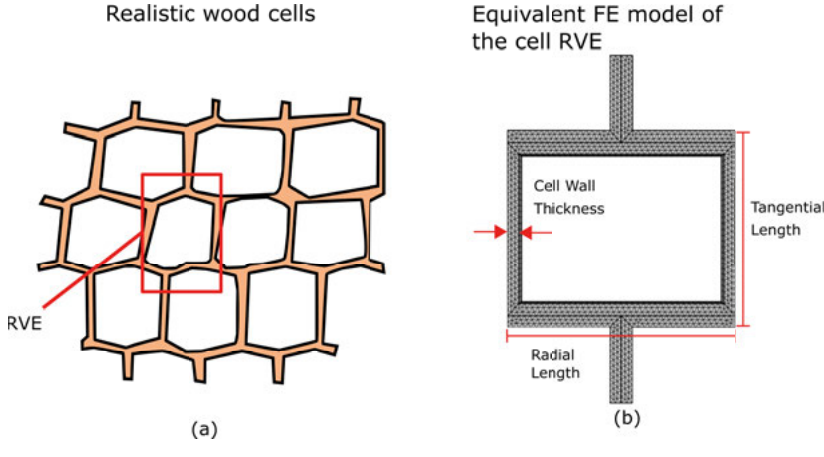

Figure 8.3. (a) A realistic image of the cross-section geometry of the Norway Spruce EW cellular tissue traced from SEM micrograph [57]. (b) Resulting FE model of the micro-scale model (single cell RVE) in this study.

The assumptions made for the models are listed below:

- For the present study, the microfibril angle (MFA) for both species is assumed to be 10 degrees, which is a typical angle measured for normal wood [58]. The angle is implemented by adjusting the material directions of the cell walls in the micro-scale model.
- It has been reported that the S2 layer of the cell wall is by far the thickest (>80%) [33, 52, 59]. To simplify the model, only the S2 layer of the cell wall was considered and modelled in the micro-scale model.
- In the microscale model, rectangular-shaped cells are modelled (see Fig. 8.3) for the sake of simplicity. A similar microstructure has also been observed in SEM micrographs [57]. This has also been assumed in elastic homogenization schemes such as in [37].

In the figures below, we can assess the performance of the multiscale model by comparison of two experimental creep tests on Norway spruce and Japanese cypress, both being softwood species. In Fig. 8.4, the three plots represent three separate creep tests, in which the loading direction is the same direction as the measured creep strain. In Fig 8.5, all three plots represent one single creep test, in which the specimen was loaded in tension in the longitudinal direction, but all three normal strains were measured to capture the Poisson's effect.

The macroscopic creep behaviour of two different species of softwood has been effectively reproduced using a multiscale linear viscoelastic model. This was made possible by considering the material structures of the softwood species and employing a uniform linear viscoelastic model for the cell wall. The parameters in the model solely pertain to the viscous behaviour of the cell wall. Remarkably, the model successfully captures general 3D creep deformations at the macroscopic level within an order of magnitude. These results underscore the significant influence of the hierarchical structure of wood on creep deformations, including factors such as the composition of earlywood (EW), latewood (LW), and rays, as well as the dimensions and spatial distribution.

The implications of these findings are noteworthy, particularly in the context of cost-effective predictions of long-term deformations. Conducting comprehensive creep testing is typically more expensive than characterizing the microstructure of materials. Therefore, the application of multiscalar viscoelastic modelling holds promise for predicting creep behaviour and can potentially provide valuable insights into macroscopic shear, which is challenging to experimentally test and lacks sufficient published data. Additionally, through parametric studies, it becomes possible to identify the key parameters that significantly impact creep resistance. This knowledge is valuable for materials selection and has the potential to guide materials modification strategies.

Moreover, the general methodology employed in this study can be extended to predict creep in other viscoelastic hierarchical materials, such as polymer composite laminates and woody plant materials like bamboo.

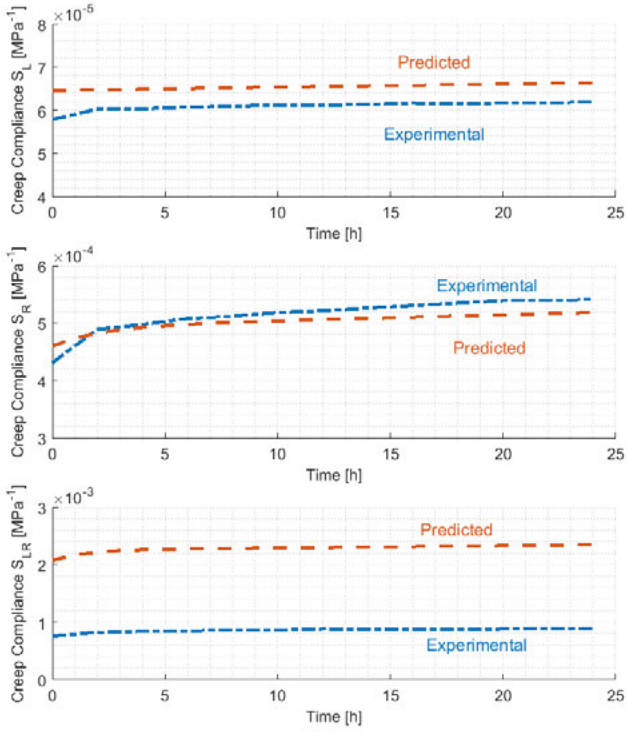

Figure 8.4. Comparison of creep compliance values for Norway Spruce from Hayashi et al. [55] and multiscale model.

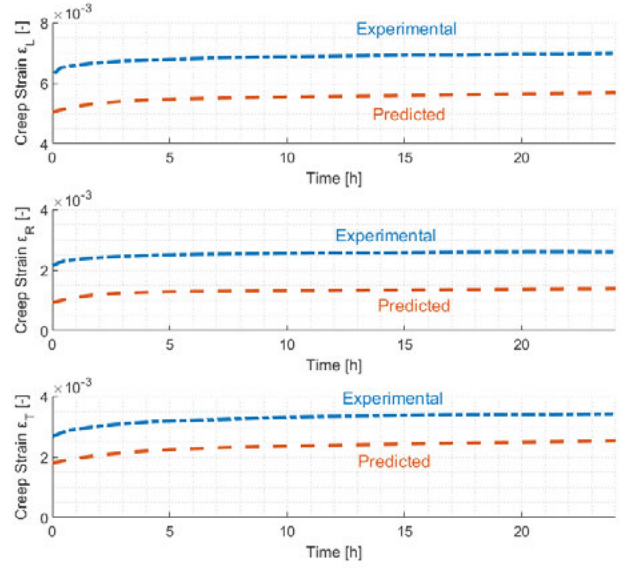

Figure 8.5. Comparison of creep strains for Japanese Cypress from Taniguchi et al. [56] and multiscale model.

9. Paper III: Characterization of shear creep using DIC on cubic samples

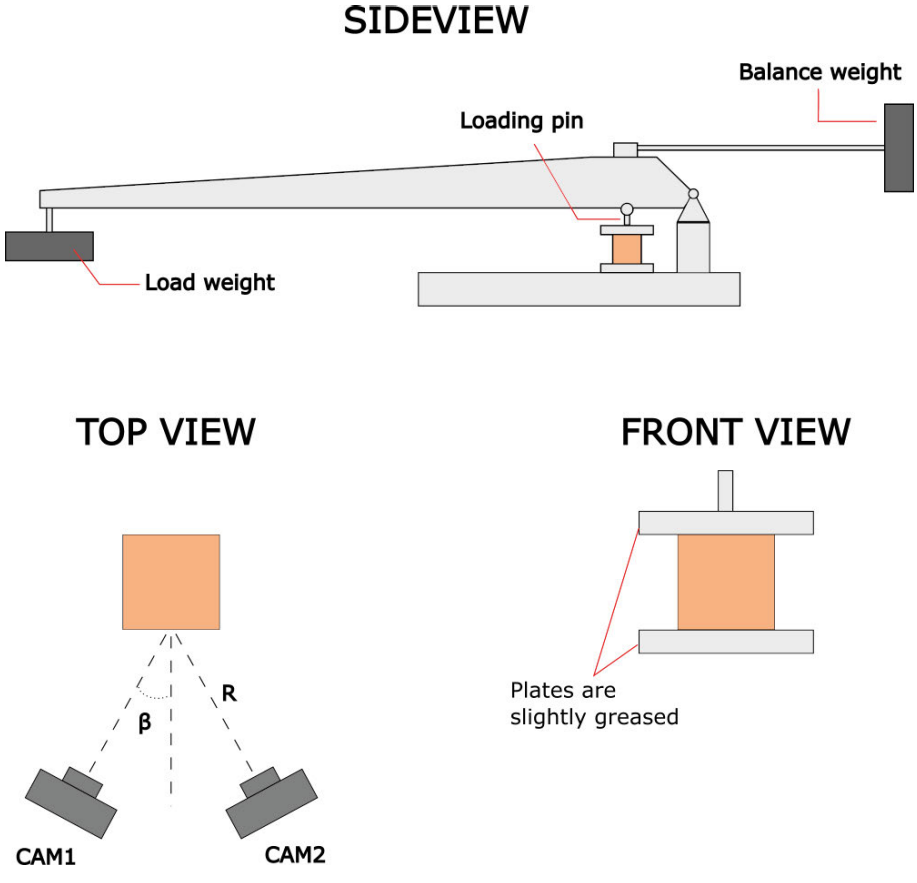

Figure 9.1. Schematic illustration of the experimental setup of Paper III. The load from the weight to the left is transferred via the jointed loading pin and then later the upper plate to compress the sample. The purpose of the balance weight is to counteract the weight of the thick beam set-up. The positioning of the cameras are defined by $\beta = 15°$ and $R = 150$ mm.

When trying to validate the material model in Paper I and the multiscale model in Paper II, experimental shear creep behaviour was not widely documented in the literature except for a few cases such as by Schniewind and Barrett [28]

and Hayashi et al. [27]. In Paper III, we introduce a straightforward testing approach utilizing uniaxial compression on wooden cubes, which is equally applicable to other types of composites. The objective is to characterize the viscoelastic shear properties of Norway spruce (Picea abies) through off-axis creep compression tests conducted in all three directions. These tests are conducted within a constant climate chamber, and the resulting creep strains are measured using digital image correlation. Although tensile testing of slender off-axis specimens would render a more uniform stress field, compression of cubic samples has the advantage of being relatively simple to carry out.

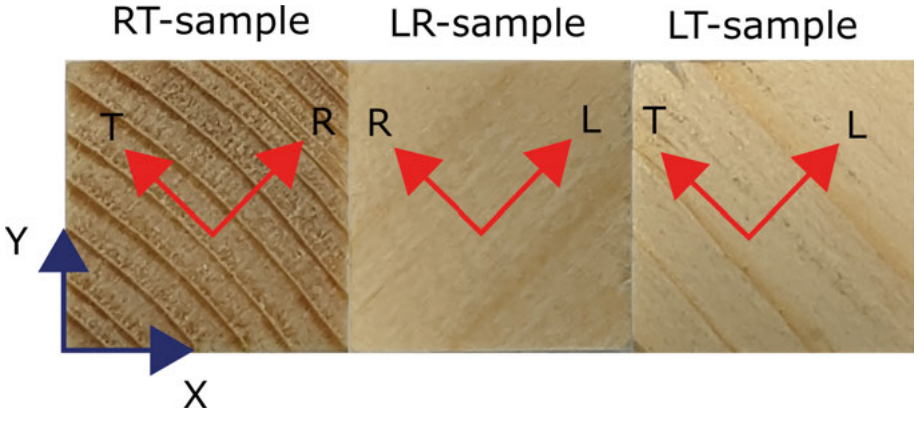

Figure 9.2. Three types of samples were prepared in Paper III. The samples were prepared in such a way that the plane of interest is rotated 45° around the global z-axis and from the global x-axis. The compression load is applied along the global y-axis.

The material directions of the samples were angled in such a way as depicted in Fig. 9.2, while the DIC measured strains were in the global coordinate system. By averaging the global strains across the surface of the sample and knowing the compressive load applied along the Y-axis, one may calculate the shear strains and shear load in the local coordinate system using well-known transformation laws. For example, for the RT samples the following equations were used:

$$\varepsilon_{\mathrm{RT}} = (\varepsilon_x - \varepsilon_y)\sin\alpha\cos\alpha + \varepsilon_{xy}\cos 2\alpha \tag{9.1}$$

$$\sigma_{\mathrm{RT}} = (\sigma_x - \sigma_y)\sin\alpha\cos\alpha + \sigma_{xy}\cos 2\alpha \tag{9.2}$$

Hence, the creep compliance J_{RT} may be derived by using the 1D relation between the evolution of creep strain and constant stress as described by the constitutive equation

$$\varepsilon(t) = J(t)\sigma_0. \tag{9.3}$$

Here, $J(t)$ is assumed to follow the behaviour of a Standard Linear Solid (SLS) model, for the sake of fitting the experimental data in this study, see Fig. 9.3

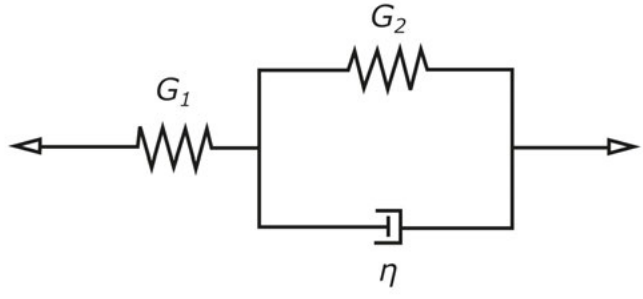

Figure 9.3. Kelvin representation of the standard linear solid model ([40]).

In total, 15 creep tests were performed, of which five were for each sample type (RT, LR and LT). The strain fields of the samples are captured every 6 minutes, which are later averaged to a scalar value to represent the overall behaviour of the sample. The samples were tested under constant climate at $65 \pm 2\%$ RH and $22 \pm 1°$C. In Fig. 9.4, the experimental creep compliance J_{RT} is plotted. The remaining experimental data for the LT and RT samples are shown in Paper III.

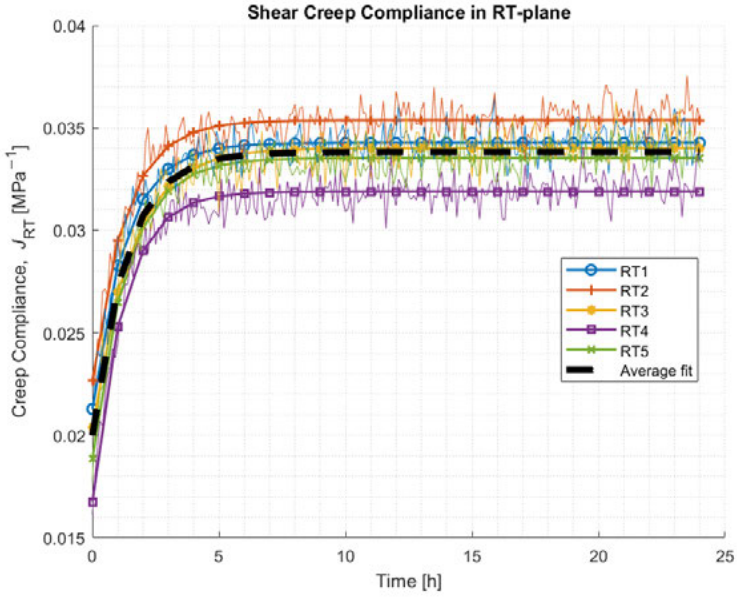

Figure 9.4. Creep compliance for five different RT samples: Measurements, fitted SLS model for each sample and in average (dashed black line).

Since the shear creep compliance for Norway Spruce is, to the knowledge of authors, not available in the literature, it is not possible to compare the curves with any independent studies. However, the elastic shear modulus determined from the instantaneous deformation when the load is applied can be compared with literature values for Norway spruce. The shear modulus values are presented in Table 9.1, and it can be seen that the measured values fall within the ranges found by other investigations.

Table 9.1. *Shear modulus values obtained at $t = 0$ for all samples. Literature value ranges for Norway Spruce are also presented, although quantified using different test methods under climate conditions ([60, 61, 62, 63, 64, 65]).*

	# 1	# 2	# 3	# 4	# 5	μ	Ref.
G_{RT} [MPa]	49.46	43.26	52.24	61.94	56.28	52.0	20.0-90.0
G_{LR} [MPa]	690.4	741.0	701.3	678.1	734.1	709.0	600.0-800.0
G_{LT} [MPa]	791.13	643.5	657.4	628.7	619.9	645.6	600.0-750.0

μ – mean value.

The authors have presented a viable creep setup to obtain the shear creep compliance of wooden samples for the RT, LR and LT planes in uniaxial compression. No intricate test jigs or equipment are required for this method, as the setup only relies on the orientation of the material directions inside the wooden cube and testing in compression. Although the method was used for Norway spruce, it is equally applicable for other types of wood species as well as other composite materials that possess orthotropic behaviour. The simplicity of the method is considered to compensate for some amount of inevitable non-uniformity in stress and deformation fields which are reduced in more complicated setups for tensile loading of slender specimens.

This study has been focused on shear creep only, motivated by a striking lack of data in the literature and the usefulness of presenting a straightforward and relative method that could be implemented in most mechanical testing laboratories. Although not well reported, there is more data on normal creep along the main material axes for wood than on shear creep. These shear creep compliance data could in principle be used in finite element models. For other rheological models than the SLS model used here, one would have to re-fit the data with the particular material model. Indeed, the creep behaviour in the normal direction of Norway Spruce is not the scope of this study, and thus the authors refer to the works of [13, 23, 25, 66] on how to extract the creep data in the normal direction, including the Poisson's behaviour during creep. After having the full 3D viscoelastic representation for a particular type of wood, it would be possible to simulate the time-dependent behaviour of wood in a constant climate.

10. Paper IV: Four-point bending creep tests on Norway spruce beam samples

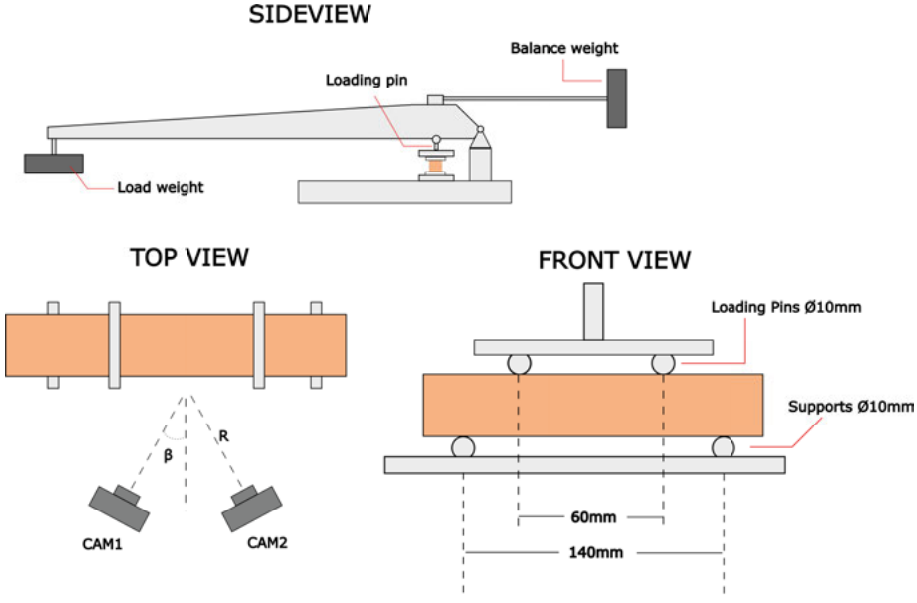

Figure 10.1. Schematic illustration of the experimental setup of this study. The load from the weight to the left is transferred via the jointed loading pin and then later to the two loading rollers/pins to bend the beam sample. The purpose of the balance weight is to counteract the weight of the steel rig itself. $L1 = 60\,\text{mm}$ and $L2 = 140\,\text{mm}$

In Paper IV, the intention was to compare the multiscale model developed in Paper II even further with the creep of a structural member. The reason is that the model was tuned against experimental creep tests at the material level, rather than at the structural level. A 4-point bending creep test was developed in Paper IV to see how the multiscale model would perform against combined loading scenarios. This enables predicting macroscopic creep behaviour based solely on microstructural parameters given in Paper II, potentially saving time and costs associated with comprehensive creep characterization in all material directions, including the relatively intractable shear loading case.

The experiments were performed in a controlled climate with relative humidity (RH) of $65 \pm 2\%$ and a temperature of $20 \pm 1\,^{\circ}\text{C}$. Fifteen samples were prepared

and machined from Norway spruce, which were locally sourced from Uppsala, Sweden. The dimensions of the beam samples were 150 x 15 x 15 mm^3. The fibre direction (L) of the wooden sample was along the length of the beam, while the radial (R) and tangential (T) directions span the cross-section of the beam angled in a 45°manner. Before testing, the samples were conditioned with the same climate conditions for three months. After conditioning, the density of the samples was measured with a value of 443 ± 43 kg/mm^3.

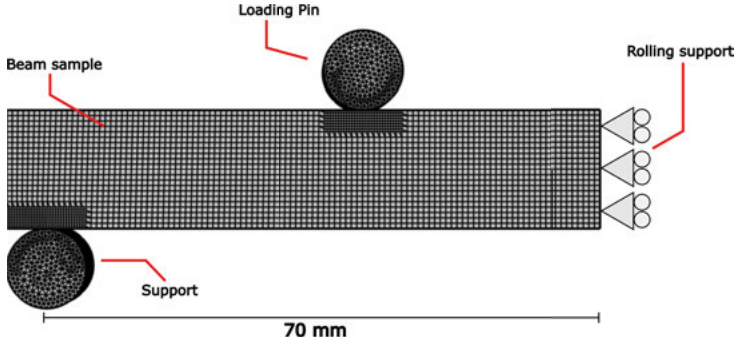

Figure 10.2. The FE model in the present study is modelled in COMSOL.

To assess the performance of the model, we compared the deflection in 24 hours and strain fields from DIC measurements to an equivalent FE model using the material parameters from the multiscale model for Norway Spruce. See Fig. 10.3

Four-point bending creep tests were conducted on Norway spruce and compared with a finite element (FE) model that utilized material parameters derived from their developed multiscale model. The qualitative comparison of strain and displacement fields, analyzed using digital image correlation (DIC), revealed satisfactory similarities. Nevertheless, there were slight variations in the longitudinal strain field, which can be attributed to the inherent wood heterogeneity that cannot be precisely replicated in the homogeneous FE model.

The comparison of displacements, as seen in Fig. 10.4 at specific points along the beams between the experimental and FE model results indicated a stiffer behaviour in the FE model, with a relative difference of approximately 20% at the end of the experiments. This suggests the need for further refinement of the multiscale model, potentially by incorporating more experimental creep data. One possible approach is to adjust the elastic material parameters, although such adjustments should be justified through additional experiments.

Additionally, another FE model was developed to emphasize the importance of shear creep. In this model, the τ parameters related to shear components (C_{44}, C_{55}, C_{66}) were set to zero. The comparison between the two FE models revealed a 6% difference in displacements at $t = 24$ hours; however, this difference could be more significant in shear-dominated scenarios.

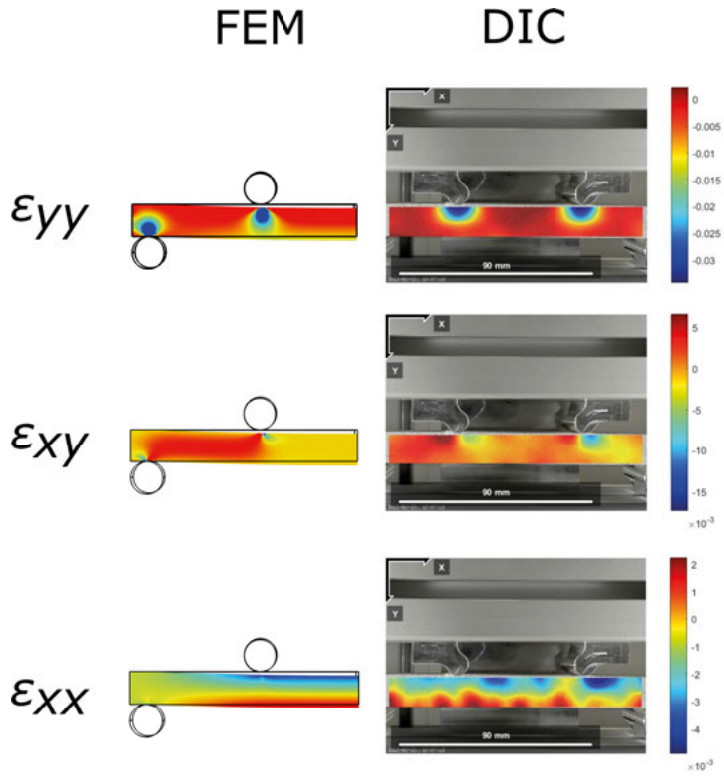

Figure 10.3. Comparison of the strain fields between FEM and experiment at $t = 24$ hours.

The methodology presented in this study, coupled with the prior work in Paper II, has the potential for application in predicting creep behaviour in other viscoelastic hierarchical materials, such as polymer composite laminates. It may offer an alternative approach to methods introduced in earlier studies [50, 51].

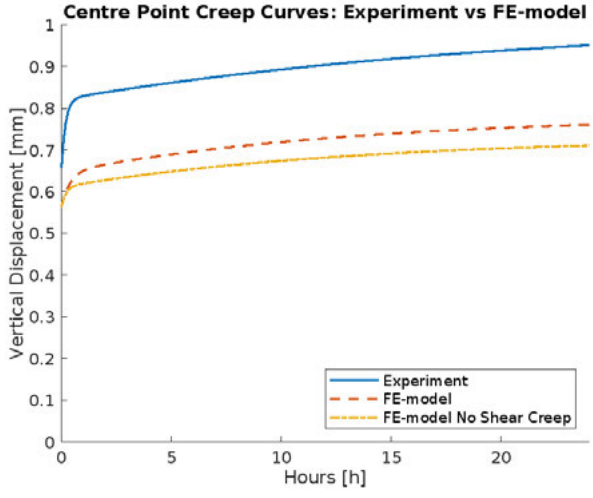

Figure 10.4. Comparison between averaged experimental data fitted against an exponential function and FE model at the centre point of the beam sample.

11. Paper V: Feasibility of wooden towers for offshore wind turbines: Creep and fatigue predictions

In Paper V, an application in larger wooden structures is explored. The World-WideWind initiative [67] has introduced the Counter Rotating Axis Floating Tilted Turbine (CRAFTT) concept, which has seen recent developments in generator design [68] and dynamics [69]. However, engineering questions arise, particularly concerning the choice of material for the wind turbine tower. Previous successful experiences with wooden towers for vertical axis wind turbines [70, 71] suggest wood as a viable alternative to traditional steel towers on land. For offshore applications with larger turbines, durability demands are more challenging.

Recent advancements in large-scale wooden buildings, like the 17-floor Mjöstarnet with a timber frame [72] and the 100-meter Hannover-Marienwerder wind turbine tower made of wood [73], provide hope for upscaling wooden tower structures. Prospects include wooden skyscrapers [74].

Offshore installations face unique challenges, including maintenance, constant water exposure, and moisture issues. A longer structural lifespan is desired to extend inspection intervals, focusing on fatigue and creep over time. Moisture presents challenges for load-bearing wooden structures, reducing stiffness, strength, and increasing creep deformations while decreasing fatigue resistance [75, 76]. To address these effects, two options exist. One approach is preventing moisture ingress with impermeable barriers. Alternatively, designers can account for moisture's impact on mechanical properties, which can be severe, in particular for high and fluctuating moisture contents. Treating the wood to make it hydrophobic is impractical due to the abundance of hydrophilic wood polymers, especially hemicellulose, in the bulk of the wood components. Through-thickness chemical impregnation is neither practical nor environmentally justifiable.

In the following, numerical studies with simpler load cases are presented when dealing with the CRAFFT concept design. A simplified vertical axis wind turbine inspired by the design presented in [68], is modelled in COMSOL (v5.6). See Fig. 11.1

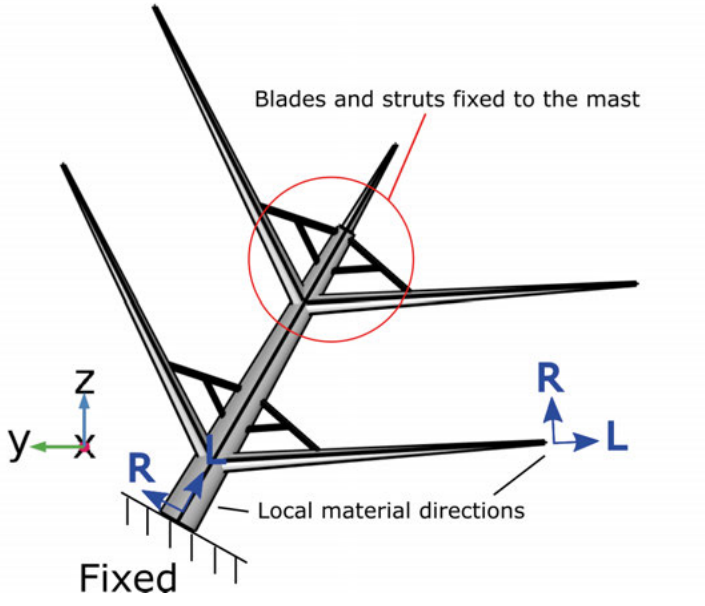

Figure 11.1. FE-model of CRAFTT, inspired from [68]. It is inclined with an angle to the ground (or sea), and both mast and blades are made from solid wood Norway spruce using the same material parameters produced in [77].

In contrast to reality, the model assumes that the blades and struts of the turbine are fixed to the mast, while the bottom of the mast is anchored to the ground. In reality, these connections and boundary conditions are generally free to rotate to some extent, using mechanisms that were considered too complex to model in initial designs like this. To account for the inherent orthotropic behaviour of wood, both the mast and blades have their local material direction, with the longitudinal behaviour of wood defined parallel to the lengths of the mast and blades. The material model and parameters are taken from [77], which presents a linear viscoelastic and linear elastic model for Norway spruce derived from a micromechanical perspective.

This study considers two load cases, as shown in Figure 11. The fatigue load case involves a static elastic analysis, where computed stresses are interpreted as stress amplitudes. These stress amplitudes can be used in conjunction with a Wöhler curve [78]. On the other hand, the creep load case entails a transient finite element analysis to capture the evolution of the total deflection of the wind turbine over 24 hours (limited to the testing time in the experimental creep characterization).

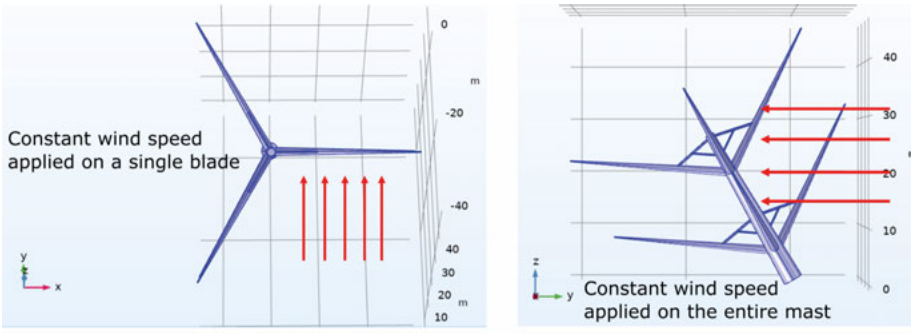

(a) Fatigue Loadcase (b) Creep Loadcase

For both load cases, a constant wind speed of 10 meters per second is considered. The resulting pressure load, P, may be calculated by approximating each body as a cylinder with the drag force equation below

$$P = \frac{1}{2} C_{\mathrm{d}} \rho_{\mathrm{air}} u^2, \tag{11.1}$$

where $C_{\mathrm{d}} = 1.2$ is the drag coefficient for a long cylinder, ρ_{air} is the density of air and u is the applied wind speed. It should be also noted that the self-weight of the tower is included in both load cases.

Due to the limited availability of fatigue data for wood species in various material directions, this study only focuses on evaluating longitudinal stresses. Wöhler curves for softwood, as referenced in [78], have been considered. However, the longitudinal stresses assessed in this study (refer to Fig. 11.2) significantly exceed the threshold given by [78]. Notably, the maximum stress observed, reaching 110 MPa near the connection between the blade and mast, indicates an immediate fatigue failure in the model.

The high-stress levels can be attributed to the over-constrained connections between the blade and mast. In future simulations, it is advisable to permit rotational degrees of freedom in these connections to more accurately reflect real-world conditions and potentially mitigate these excessively high stresses. For a properly designed joint with a well-mitigated stress concentration, one can look further away from the inevitable stress concentrations at the joints by just 5-10 elements and one can find stresses at the 30-40 MPa region, which is below the endurance limit threshold according to the Wohler curve given by [78]. This method is common when performing stress assessments of FE-models of welded structures [79], which can be applicable here, but needs further development on what assumptions can be made.

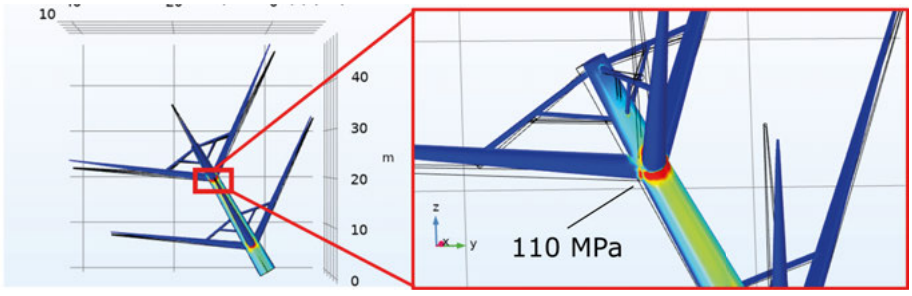

Figure 11.2. Maximum longitudinal stress of 110 MPa is found beneath the blade for the fatigue load case.

In the transient analysis, the total deflection of the tip was tracked over 24 hours for demonstration purposes, see Fig. 11.3. It was observed that the deflection increased from an initial elastic deflection of 0.336 mm to a maximum value of 0.354 mm after 24 hours. These are negligible and not even measurable deflections. Even if the creep predictions are extrapolated for a couple of decades, the displacement will be very limited. The fatigue loading case is thus considered to be of higher importance than creep in this application.

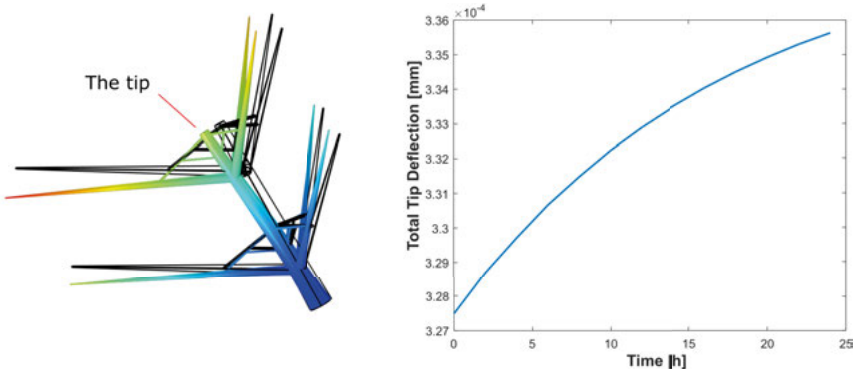

Figure 11.3. Deflection of the wind turbine tip is followed in 24 hours due to the creep load case.

Part IV:

Conclusions and outlook

The thesis deals with the static and, in particular, time-dependent mechanical properties of wood. This study ties creep from cell-wall of wood up to structures, which includes experiments and numerical work. A material model is formulated appropriate for orthotropy such as wood, which is used as a foundation for subsequent work in this thesis. A relationship between microstructural parameters to macroscopic properties is formulated by the multiscale model and may be used not only for Norway spruce but also for other types of softwood by modifying the geometrical parameters. Since shear creep is not well documented for wood in the literature, methods have been developed in the thesis to contribute more data regarding this topic. This includes the multiscale model, but also an experimental off-axis compression procedure on the material level. Thereafter, the thesis proceeds to go into higher length scales using the 4-point bending test and also to demonstrate how the results may be used in a larger wooden structure such as the CRAFTT wind turbine. Although the results need further verification due to the lack of experimental data on wooden wind turbine structures, it may prove useful in the future as a starting point on how to simulate creep behaviour in such structures. In any case, the preliminary structural predictions indicate that wood can be considered a load-carrying material in large-scale offshore wind turbines, just like what has been seen in recent years for multi-storey buildings.

Conclusions

A material model for linear viscoelasticity is presented in the thesis which manages to capture the full 3D behavior of an orthotropic material, such as wood. Regarding the material model, two cases are considered, where (i) Poisson's ratios are time-dependent, and (ii) Poisson's ratios are constant and do not vary with time. However, in Paper I, a relatively poor match was found when the Poisson's ratios were set to be constant. Thus this assumption of constant Poisson's ratio should be made with caution.

In addition to constitutive modelling, a multiscale model was developed whose sole purpose was to predict the linear viscoelastic behaviour of softwoods. An advantage can be seen using the anisotropic material model developed in Paper I, which shows that going over multiple scales in wood, leads to orthotropic behaviour at each scale. The model starts by using geometrical parameters on the cell and tissue levels which are different for different softwood species, and then using computational homogenisation to upscale the properties. The main assumption in Paper II was that softwood species roughly share the same constituents and ultrastructure at the cell wall scale, meaning that material properties of the cell walls were assumed to be the same between species. Essentially the difference on material level is attributed to the differences in material structure rather than differences in the cell-wall properties. Further simplifications were also made in the multiscale model; one being that the cell wall is entirely composed of one layer (the S2 layer, which comprises 80% of the entire wall) and the other being that the geometrical shape of the cells is rectangular. In Paper II, the model attempts to reproduce the macroscopic creep behaviour of two different species of softwood, with ostensibly encouraging results. The model captures the general 3D creep deformation at the macro scale within an order of magnitude, but still, there are some slight differences. However, the implications of these findings are important in the context of cost-effective predictions of long-term deformations, which are noteworthy when trying to observe the time-dependent behaviour of orthotropic materials. Moreover, the general methodology employed in this study can be extended to predict creep in other viscoelastic hierarchical materials, such as polymer composite laminates and bamboo.

Due to the striking lack of shear creep data for wood in the literature, a shear creep test has been developed and presented in this thesis. It is based on a straightforward approach using uniaxial compression on wooden cubes but is equally applicable to other types of composites. In Paper III, we characterized the viscoelastic shear creep properties of Norway spruce through DIC for all three shear planes. The data was fitted against an SLS model, making it feasible to report the results in the form of model parameters. These data are allegedly the first of its kind, and can therefore not be compared with other independent studies at this point. The elastic shear modulus values captured

during the experiment were used instead for comparison, and it was seen that the measured values fall within the ranges found by other investigations. Using these results, finite element modelling of wood may be improved, in which shear creep is often neglected in structural predictions. It should be noted that the compression of cubic samples is hampered by a non-uniform stress field (barreling effect). On the other hand, this simple test method has the advantage of being relatively practical and uncomplicated, with the possibility of testing multiple directions in the same sample.

A 4-point bending creep test on Norway spruce beams was conducted to compare the results with a finite element model that used the output material parameters from the multiscale model in Paper II. A qualitative comparison was made by comparing the strain and displacement fields at the end of the test, with satisfactory similarities. However, there were slight differences in the longitudinal strains along the beam samples, which could be attributed to the inherent heterogeneity of wood that was not accurately replicated in the homogeneous FE model. Moreover, quantitative measurements were done by comparing the vertical displacements along the beam, which revealed a stiffer behaviour in the FE model, with a relative difference of 20% at the end of the experiment. This suggests that further tuning of the multiscale model is required, either by tuning the moisture-dependent material parameters at the cell wall even further or by applying more realistic features in the multiscale model, such as a more accurate representation of the cells or adding the additional layers of the cell walls. In addition to the aforementioned comparisons in Paper IV, another FE model was conceived using modified material parameters to compare with the experiments. In this case, the material parameters were altered in such a way that no creep would occur in the shearing direction. In other words, it would just behave elastically in shear. The comparison between the two FE models showed a 6% difference in displacements after 24 hours; however, this difference could be more pronounced in shear-dominated problems, e.g. allowing the outer spans in the 4-point bending test to be longer. In general, it is concluded that it is not safe to neglect shear creep in wood structures. The full creep model was further employed to predict deformation in a wind turbine tower. In this particular case, the creep deformations were found to be small, and fatigue was found to be of higher importance.

With further refinements to the multiscale model, it should in principle be feasible to obtain a comprehensive 3D viscoelastic representation for any given wood species starting by modeling the constituents that are common for all species. This approach has the potential to save time and costs associated with extensive creep characterization in all material directions. The methodology presented in this thesis could potentially also be applied to predict creep in other viscoelastic hierarchical materials, such as polymer composite laminates. It may serve as an alternative method to those introduced in previous studies [50, 51].

Outlook

In this thesis, the constitutive modelling has been constricted to only linear elastic and linear viscoelastic behaviour in the introduced models. In many works on wood mechanics such as [5, 20, 21, 22, 80], other types of behaviour are usually modelled including mechanosorptive creep and hydro expansion. These phenomena all stem from the moisture-dependent physics of wood that has not been included in this study. Therefore, the results and models produced in Papers I to IV, are strictly confined within the bounds of constant climate. Thus, it would be of great interest to generalize predictions of moisture-induced strains using a similar micromechanical approach as here, for a more complete and practical use. To the knowledge of the authors, there are no studies in the literature about multiscale models of mechanosorptive behaviour in wood. Future studies may include cell walls which present four deformation mechanism

$$\varepsilon_{ij} = \varepsilon_{ij}^{\mathrm{e}} + \varepsilon_{ij}^{\mathrm{h}} + \varepsilon_{ij}^{\mathrm{ve}} + \varepsilon_{ij}^{\mathrm{ms}} \tag{11.2}$$

where, ε_{ij}^{e} is the elastic strain, ε_{ij}^{h} is the hygroexpansion strain, ε_{ij}^{ve} is the viscoelastic strain and finally ε_{ij}^{ms} is the mechanosorptive strain. The upscaling from cell wall scale (micro) to macroscale, is possible by employing computational homogenization using periodic boundary conditions and the Hill-Mandel lemma:

$$\langle \sigma_{ij}^{\mathrm{micro}}(\mathbf{x}) : \varepsilon_{ij}^{\mathrm{micro}}(\mathbf{x}) \rangle = \sigma_{ij}^{\mathrm{macro}} : \varepsilon_{ij}^{\mathrm{macro}} \tag{11.3}$$

which expresses the equivalence between the average microscopic (cell wall) energy and the macroscopic energy. Using the proposed cell wall and the principles of homogenization might reveal the macroscopic behaviour for the overall deformation mechanics in wood, including both mechanosorption and viscoelasticity. Regardless, with the common assumption of additive decomposition of strain, the conclusions made from just working with linear elastic and linear viscoelastic strains may still hold when adding additional strains in the multiscale model, since the different strains are assumed not to be correlated with each other in small deformation theory.

Since a limitation in the present study is the assumption of constant climate, it is suitable to apply the results in applications in which the climate is practically constant. In addition to the application of the wind turbines as done in Paper V, one suggestion would be for example cultural heritage, i.e. the Vasa ship [25, 39, 81]. The analysis of the measurements showed that the ship undergoes continuous deformations with increasing strains, which may be dangerous for structural stability in the future.

Overall, since wood is expected to be used more in the future, being a renewable material, and structures made thereof ought to have longer lifetimes,

research on the long-term creep of wood is considered important. The work presented in this thesis is limited to some small steps facilitating this transition. A broad front of targeted research is needed to pave the way for more efficient use of wood in long-standing structures, from a wide variety of scientific and engineering disciplines. One important area is creep, where more efficient models, characterization methods and design tools can contribute to realizing the full potential of wood as load-carrying material. The ideas in the present thesis could be refined, validated, improved and eventually put into practical use.

Summary in Swedish

Denna avhandling bidrar till att ge en inblick i de invecklade mekaniska egenskaperna hos naturmaterial, med särskild tonvikt på trä. Trots årtusenden av praktisk användning av trä som konstruktionsmaterial så är förståelsen av samband mellan struktur och lastbärande egenskaper fortfarande relativt begränsad. Det beror på beror bland annat på materialets komplexa struktur, naturliga variation, olinjära beteende och känslighet för förändringar i fukthalt. Med en bättre mekanisk förståelse för trämaterial så kan man utveckla bättre metoder för att konstruera med trä som lastbärande material.

Trä och liknande biobaserade naturmaterial har en enorm potential på grund av deras relativa kostnadseffektivitet, miljövänlighet, förnybarhet, användarvänlighet inom konstruktion, liksom deras återanvändbarhet. Trä har enastående styvhet och styrka längs fibrerna och överträffar många konstgjorda konstruktionsmaterial när det gäller styrka och styvhet i förhållande till vikten. En inneboende egenskap är att trä är anisotropt, dvs. det har olika egenskaper i olika riktningar. Därför måste flera parametrar beaktas för en noggrann karaktärisering.

Trä är till sin natur ett heterogent material, vilket leder till betydande rumsliga variationer i lokala spänningar och deformationer under belastning. Ett sätt att hantera samband mellan mikrostrukturella heterogeniteter på makroskopiskt mätbara fenomen är matematiska homogeniseringsmetoder. Sådana har varit etablerade sedan 1970-talet, funnit användning inom materialmekanik för bland annat fiberkompositer och trä.

Under de senaste åren har det uppkommit ett ökat intresse för det viskoelastiska beteendet hos kompositer och trästrukturer. Det beror på betydelsen av materialens långvariga användning i lastbärande tillämpningar där tids-

beroende deformationer normalt uppstår. De flesta undersökningarna har utforskat relationen mellan träets mikrostruktur och dess momentana elastiska egenskaper, och långt färre studier har utforskat kopplingen mellan mikrostruktur och dess tidsberoende viskoelastiska egenskaper.

Avhandlingen fokuserar på de statiska och tidsberoende mekaniska egenskaperna hos trämaterial, specifikt krypning, dvs. deformation till följd av konstant belastning. Idén är att utgå från cellväggskryp och prediktera krypning i trämaterialet och i strukturer. Studien inkluderar omfattande experiment och numeriskt arbete, vilket lett fram till en materialmodell som är lämplig för ortotropa och heterogena material som trä. Den multiskalära modellen möjliggör en koppling mellan mikrostrukturella parametrar och makroskopiska krypegenskaper, vilket potentiellt kan tillämpas på olika barrträdslag.

Data för krypning hos trä i normalriktningarna finns dokumenterad, men för just skjuvkrypning saknas experimentella resultat i litteraturen. Denna kunskapslucka föranleder utveckling av en relativt enkel mätmetod att karakterisera skjuvkrypning. En komplett krypkarakterisering i samtliga belastningsriktningar är nödvändig för att kunna förutsäga deformationer i de flesta träkonstruktioner.

Vidare visar avhandlingen hur resultaten från experiment på materialnivå och materialmodeller kan tillämpas på större träkonstruktioner, t.ex. på lutande torn till havsbaserade vindturbiner. Resultat kräver ytterligare validering, men visar ändå potentialen att kunna simulera krypbeteende i större konstruktioner.

Sammanfattningsvis belyser avhandlingen den trämaterialens komplexitet och några av de förenklande antaganden som bör göras för att utveckla modeller nödvändiga för praktisk användning av trä som konstruktionsmaterial. Resultaten ger förhoppningsvis värdefulla bidrag som i slutändan kan effektivisera användningen av trä i lastbärande strukturer. För att nå dithän är fortsatt forskning inom detta område av vikt. Speciellt mekanosorptiva egenskaper och fuktrelaterade deformationer bör undersökas, och tillämpas i olika områden som kulturarv och nya hållbarare konstruktion. Genom att fortsätta förbättra modellerna och metoderna som presenterats här kan framtida forskning leda till ännu mer effektiv användning av trä i långvariga och hållbara konstruktioner.

Acknowledgements

I would like to express my heartfelt gratitude to the individuals who have played a pivotal role in my Ph.D. journey, without whom this achievement would not have been possible.

First and foremost, I extend my deepest appreciation to my main supervisor, Professor Kristofer Gamstedt. Your unwavering support, guidance, and profound insights have been instrumental in shaping my research and academic growth. Your mentorship has been invaluable, and I am immensely grateful for the trust you placed in me throughout this journey.

I would also like to acknowledge the invaluable contributions of my co-supervisors. Dr. Mahmoud Mousavi, your expertise in computational aspects has been pivotal in enhancing the depth and rigour of my research. Your patience and willingness to share your knowledge have been immensely beneficial. I extend my sincere thanks to Dr. Reza Afshar for your invaluable assistance on the experimental side of my project. Your dedication to precision and your willingness to share your expertise have significantly enriched the quality of my research.

I am deeply grateful to my fellow Ph.D. students, Marie, Klara, Parnian, Salim, and Danial, for their unwavering camaraderie, support, and valuable discussions that enriched my research experience and made the journey memorable.

I am also thankful to the entire academic and administrative staff at Uppsala University for providing a conducive research environment and resources that supported my Ph.D. journey.

My heartfelt thanks go out to my friends and family for their unwavering support, encouragement, and understanding throughout this demanding endeavour.

Finally, I am thankful to the research community and all the participants who contributed to the body of knowledge in my field, as their work has been a constant source of inspiration and motivation.

This Ph.D. journey has been a transformative experience, and I am deeply appreciative of the guidance, support, and inspiration provided by all those who have been a part of it. Thank you for being a part of this incredible voyage.

References

[1] L. Barham, G. Duller, I. Candy, C. Scott, C. Cartwright, J. Peterson, C. Kabukcu, M. Chapot, F. Melia, V. Rots, *et al.*, "Evidence for the earliest structural use of wood at least 476,000 years ago," *Nature*, pp. 1–5, 2023.

[2] S. Holmberg, K. Persson, and H. Petersson, "Nonlinear mechanical behaviour and analysis of wood and fibre materials," *Computers & structures*, vol. 72, no. 4-5, pp. 459–480, 1999.

[3] L. Bach, *Nonlinear mechanical behavior of wood in longitudinal tension*. State University of New York College of Environmental Science and Forestry, 1966.

[4] B. D. Kristian, "Mechanical properties of clear wood from norway spruce," 2009.

[5] S. Florisson, *Moisture-induced stress and distortion of wood: A numerical and experimental study of wood's drying and long-term behaviour*. PhD thesis, Linnaeus University Press, 2021.

[6] S. Huč and S. Svensson, "Coupled two-dimensional modeling of viscoelastic creep of wood," *Wood science and technology*, vol. 52, no. 1, pp. 29–43, 2018b.

[7] A. Ranta-Maunus, "The viscoelasticity of wood at varying moisture content," *Wood science and technology*, vol. 9, no. 3, pp. 189–205, 1975.

[8] R. H. Falk, "Wood as a sustainable building material," *Forest products journal. Vol. 59, no. 9 (Sept. 2009): pages 6-12.*, vol. 59, no. 9, pp. 6–12, 2009.

[9] SwedishWood, "Wood construction cuts climate footprint," 2020.

[10] G. Wimmers, "Wood: a construction material for tall buildings," *Nature Reviews Materials*, vol. 2, no. 12, pp. 1–2, 2017.

[11] M. F. Ashby, L. Gibson, U. Wegst, and R. Olive, "The mechanical properties of natural materials. i. material property charts," *Proceedings of the Royal Society of London. Series A: Mathematical and Physical Sciences*, vol. 450, no. 1938, pp. 123–140, 1995.

[12] S. Cowin, "On the strength anisotropy of bone and wood," 1979.

[13] T. Ozyhar, S. Hering, and P. Niemz, "Viscoelastic characterization of wood: Time dependence of the orthotropic compliance in tension and compression," *Journal of Rheology*, vol. 57, no. 2, pp. 699–717, 2013.

[14] B. J. Zobel and J. P. Van Buijtenen, *Wood variation: its causes and control*. Springer Science & Business Media, 2012.

[15] P. Castéra and P. Morlier, "Variability of the mechanical properties of wood: Randomness and determinism," *Probabilities and Materials: Tests, Models and Applications*, pp. 109–118, 1994.

[16] M. A. A. Alrubaie, D. J. Gardner, and R. A. Lopez-Anido, "Modeling the long-term deformation of a geodesic spherical frame structure made from wood plastic composite lumber," *Applied Sciences*, vol. 10, no. 14, p. 5017, 2020.

[17] P. Morlier, *Creep in timber structures*. CRC Press, 1994.

[18] S. M. Holzer, J. R. Loferski, and D. A. Dillard, "A review of creep in wood: concepts relevant to develop long-term behavior predictions for wood structures," *Wood and Fiber Science*, vol. 21, no. 4, pp. 376–392, 1989.

[19] R. Afshar, M. Cheylan, and E. Gamstedt, "Creep in oak material from the vasa ship: verification of linear viscoelasticity and identifcation of stress thresholds," *European Journal of Wood and Wood Products*, vol. 78, 2020.

[20] S. Ormarsson, O. Dahlblom, and H. Petersson, "A numerical study of the shape stability of sawn timber subjected to moisture variation part 1: Theory," *Wood Science and Technology*, vol. 32, pp. 325–334, 1998.

[21] S. Fortino, F. Mirianon, and T. Toratti, "A 3d moisture-stress fem analysis for time dependent problems in timber structures," *Mechanics of time-dependent materials*, vol. 13, no. 4, pp. 333–356, 2009.

[22] M. M. Hassani, F. K. Wittel, S. Hering, and H. J. Herrmann, "Rheological model for wood," *Computer Methods in Applied Mechanics and Engineering*, vol. 283, pp. 1032–1060, 2015.

[23] J. Jiang, B. E. Valentine, J. Lu, and P. Niemz, "Time dependence of the orthotropic compression young's moduli and poisson's ratios of chinese fir wood," *Holzforschung*, vol. 70, no. 11, pp. 1093–1101, 2016.

[24] R. Afshar, "Characterisation of mechanical properties of wood: Size effect," in *Theoretical Analyses, Computations, and Experiments of Multiscale Materials*, pp. 659–669, Springer, 2022.

[25] A. Vorobyev, *Static and time-dependent mechanical behaviour of preserved archaeological wood: Case studies of the seventeenth century warship Vasa*. PhD thesis, Acta Universitatis Upsaliensis, 2017.

[26] A. Vorobyev, I. Bjurhager, N. P. van Dijk, and E. K. Gamstedt, "Effects of barrelling during axial compressive tests of cubic samples with isotropic, transversely isotropic and orthotropic elastic properties," *Composites Science and Technology*, vol. 137, pp. 1–8, 2016.

[27] K. Hayashi, B. Felix, and C. Le Govic, "Wood viscoelastic compliance determination with special attention to measurement problems," *Materials and Structures*, vol. 26, no. 6, pp. 370–376, 1993.

[28] A. P. Schniewind and J. Barrett, "Wood as a linear orthotropic viscoelastic material," *Wood Science and Technology*, vol. 6, no. 1, pp. 43–57, 1972.

[29] M. P. Ansell, "Wood microstructure–a cellular composite," in *Wood Composites*, pp. 3–26, Elsevier, 2015.

[30] D. W. Green, J. E. Winandy, and D. E. Kretschmann, "Mechanical properties of wood," in *Wood handbook: wood as an engineering material*, vol. 113, pp. 4.1–4.45, Forest Products Laboratory, 1999.

[31] A. Bensoussan, J.-L. Lions, and G. Papanicolaou, *Asymptotic analysis for periodic structures*, vol. 374. American Mathematical Soc., 2011.

[32] S. Holmberg, K. Persson, and H. Petersson, "Nonlinear mechanical behaviour and analysis of wood and fibre materials," *Computers & structures*, vol. 72, no. 4-5, pp. 459–480, 1999.

[33] K. Persson, *Micromechanical modelling of wood and fibre properties*. PhD thesis, Lund University, 2000.

[34] R. Davalos-Sotelo, "Determination of elastic properties of clear wood by the homogenization method in two dimensions," *Wood science and technology*, vol. 39, no. 5, pp. 385–417, 2005.

[35] A. Rafsanjani, D. Derome, and J. Carmeliet, "Poromechanical modeling of moisture induced swelling anisotropy in cellular tissues of softwoods," *RSC Advances*, vol. 5, no. 5, pp. 3560–3566, 2015.

[36] U. Watanabe, M. Norimoto, and T. Morooka, "Cell wall thickness and tangential young's modulus in coniferous early wood," *Journal of wood science*, vol. 46, no. 2, pp. 109–114, 2000.

[37] D. Torres-Torres, J. A. Torres, and A. García-García, "Finite element simulation based-on atomic force microscopy and nanoindentation for spruce wood microstructure analysis," *Microscopy Research and Technique*, vol. 82, no. 5, pp. 507–516, 2019.

[38] A. J. Panshin, C. d. Zeeuw, *et al.*, "Textbook of wood technology. volume i. structure, identification, uses, and properties of the commercial woods of the united states and canada.," *Textbook of wood technology. Volume I. Structure, identification, uses, and properties of the commercial woods of the United States and Canada.*, no. 3rd ed., 1970.

[39] R. Afshar, N. Alavyoon, A. Ahlgren, and E. K. Gamstedt, "Full scale finite element modelling and analysis of the 17th-century warship vasa: A methodological approach and preliminary results," *Engineering Structures*, vol. 231, p. 111765, 2021.

[40] N. W. Tschoegl, *The phenomenological theory of linear viscoelastic behavior: an introduction*. Springer Science & Business Media, 2012.

[41] N. S. Ottosen and M. Ristinmaa, *The mechanics of constitutive modeling*. Elsevier, 2005.

[42] S. R. White and Y. K. Kim, "Process-induced residual stress analysis of as4/3501-6 composite material," *Mechanics of Composite Materials and Structures an International Journal*, vol. 5, no. 2, pp. 153–186, 1998.

[43] M. A. Zocher and S. E. Groves, "A three-dimensional finite element formulation for thermoviscoelastic orthotropic media," *International Journal of Numerical Methods and Engineering*, vol. 40, pp. 2267–2288, 1997.

[44] J. Yvonnet, *Computational homogenization of heterogeneous materials with finite elements*, vol. 258. Springer, 2019.

[45] A. Tran, J. Yvonnet, Q.-C. He, C. Toulemonde, and J. Sanahuja, "A simple computational homogenization method for structures made of linear heterogeneous viscoelastic materials," *Computer Methods in Applied Mechanics and Engineering*, vol. 200, no. 45-46, pp. 2956–2970, 2011.

[46] Z. Hashin, "Viscoelastic behavior of heterogeneous media," *Journal of Applied Mechanics, Transactions ASME 32*, pp. 630–636, 1965.

[47] Z. Hashin, "Complex moduli of viscoelastic composites i. general theory and application to particulate composites," *International Journal of Solids and Structures*, vol. 6, no. 5, pp. 539–552, 1970.

[48] T. Ozyhar, S. Hering, and P. Niemz, "Viscoelastic characterization of wood: Time dependence of the orthotropic compliance in tension and compression," *Journal of Rheology*, vol. 57, pp. 699–718, 2013.

[49] V. T. Endo and J. C. de Carvalho Pereira, "Linear orthotropic viscoelasticity model for fiber reinforced thermoplastic material based on Prony series," *Mechanics of Time Dependent Material*, vol. 21, pp. 199–221, 2017.

[50] T. Matsuda and Y. Fukuta, "Multi-scale creep analysis of angle-ply cfrp laminates based on a homogenization theory," *Journal of Solid Mechanics and Materials Engineering*, vol. 4, no. 11, pp. 1664–1672, 2010.

[51] A. Sayyidmousavi, H. Bougherara, and Z. Fawaz, "The role of viscoelasticity on the fatigue of angle-ply polymer matrix composites at high and room temperatures-a micromechanical approach," *Applied Composite Materials*, vol. 22, no. 3, pp. 307–321, 2015.

[52] J. Eitelberger, T. K. Bader, K. de Borst, and A. Jäger, "Multiscale prediction of viscoelastic properties of softwood under constant climatic conditions," *Computational Materials Science*, vol. 55, pp. 303–312, 2012.

[53] Z. Lou, X. Han, J. Liu, Q. Ma, H. Yan, C. Yuan, L. Yang, H. Han, F. Weng, and Y. Li, "Nano-fe3o4/bamboo bundles/phenolic resin oriented recombination ternary composite with enhanced multiple functions," *Composites Part B: Engineering*, vol. 226, p. 109335, 2021.

[54] T. Gangwar and D. Schillinger, "Microimaging-informed continuum micromechanics accurately predicts macroscopic stiffness and strength properties of hierarchical plant culm materials," *Mechanics of Materials*, vol. 130, pp. 39–57, 2019.

[55] K. Hayashi, B. Felix, and C. Le Govic, "Wood viscoelastic compliance determination with special attention to measurement problems," *Materials and Structures*, vol. 26, pp. 370–386, 1993.

[56] Y. Taniguchi, K. Ando, and H. Yamamoto, "Determination of three-dimensional viscoelastic compliance in wood by tensile creep test," *Journal of Wood Science*, vol. 56, no. 1, pp. 82–84, 2010.

[57] A. Rafsanjani, D. Derome, and J. Carmeliet, "The role of geometrical disorder on swelling anisotropy of cellular solids," *Mechanics of Materials*, vol. 55, pp. 49–59, 2012.

[58] R. Cristian Neagu, E. Kristofer Gamstedt, S. L. Bardage, and M. Lindström, "Ultrastructural features affecting mechanical properties of wood fibres," *Wood Material Science and Engineering*, vol. 1, no. 3-4, pp. 146–170, 2006.

[59] J. Konnerth, N. Gierlinger, J. Keckes, and W. Gindl, "Actual versus apparent within cell wall variability of nanoindentation results from wood cell walls related to cellulose microfibril angle," *Journal of Materials Science*, vol. 44, no. 16, pp. 4399–4406, 2009.

[60] D. Keunecke, W. Sonderegger, K. Pereteanu, T. Lüthi, and P. Niemz, "Determination of young's and shear moduli of common yew and norway spruce by means of ultrasonic waves," *Wood science and technology*, vol. 41, no. 4, pp. 309–327, 2007.

[61] T. Ehrhart and R. Brandner, "Rolling shear: Test configurations and properties of some european soft-and hardwood species," *Engineering Structures*, vol. 172, pp. 554–572, 2018.

[62] A. Karakoç, P. Tukiainen, J. Freund, and M. Hughes, "Experiments on the effective compliance in the radial–tangential plane of norway spruce," *Composite Structures*, vol. 102, pp. 287–293, 2013.

[63] K. B. Dahl and K. Malo, "Linear shear properties of spruce softwood," *Wood science and technology*, vol. 43, no. 5, pp. 499–525, 2009.

[64] A. Sretenovic, U. Müller, W. Gindl, and A. Teischinger, "New shear assay for the simultaneous determination of shear strength and shear modulus in solid wood: finite element modeling and experimental results," *Wood and fiber science*, pp. 302–310, 2004.

[65] K. Persson, *Micromechanical modelling of wood and fibre properties*. Lund University, Department of Mechanics and Materials Lund, Sweden, 2000.

[66] R. Afshar, M. Cheylan, G. Almkvist, A. Ahlgren, and E. K. Gamstedt, "Creep in oak material from the vasa ship: verification of linear viscoelasticity and identification of stress thresholds," *European Journal of Wood and Wood Products*, vol. 78, no. 6, pp. 1095–1103, 2020.

[67] WordWideWind, "Wordwidewind." `https://worldwidewind.no/`, 2023.

[68] I. Simonsson, S. Eriksson, and H. Bernhoff, "Design and simulation of a 40 mw pm generator for the craft concept," in *Proc. EERA DeepWind Conference*, (Trondheim, Norway), 2023.

[69] L. Goude and B. Hedlund Peters, "Dynamics of a craft: A simulation study on a counter rotating vertical axis floating tilting wind turbine," 2023.

[70] E. Möllerström, F. Ottermo, J. Hylander, and H. Bernhoff *Wind Energy*, vol. 28, p. 277, 2014.

[71] S. Apelfröjd, S. Eriksson, and H. Bernhoff, "A review of research on large scale modern vertical axis wind turbines at uppsala university," *Energies*, vol. 9, p. 570, 2016.

[72] R. Abrahamsen, "Mjøstårnet - construction of an 81 m tall timber building." Internationales Holzbau-Forum IHF, 2017.

[73] TimberCompositeTechnology, "Timbercompositetechnology." `https://ticomtec.de/referenzen/timbertower-sonderkonstruktiondeutschland/`.

[74] E. Niiler, "Wooden skyscrapers are on the rise," *Wall Street Journal*, 2022.

[75] J. Wang, X. Cao, and H. Liu, "A review of the long-term effects of humidity on the mechanical properties of wood and wood-based products," *European Journal of Wood and Wood Products*, vol. 79, pp. 245–259, 2021.

[76] C. C. Gerhards, "Effect of moisture content and temperature on the mechanical properties of wood: an analysis of immediate effects," *Wood and Fiber Science*, pp. 4–36, 1982.

[77] R. Bengtsson, M. Mousavi, R. Afshar, and E. K. Gamstedt, "Viscoelastic behavior of softwood based on a multiscale computational homogenization," *Mechanics of Materials*, vol. 179, p. 104586, 2023.

[78] M. N. Yildirim, B. Uysal, A. Ozcifci, and A. H. Ertas, "Determination of fatigue and static strength of scots pine and beech wood," *Wood Res*, vol. 60, no. 4, pp. 679–686, 2015.

[79] E. Niemi, W. Fricke, and S. J. Maddox, *Fatigue analysis of welded components: Designer's guide to the structural hot-spot stress approach*. Woodhead Publishing, 2006.

[80] S. Ormarsson, O. Dahlblom, and M. Johansson, "Numerical study of how creep and progressive stiffening affect the growth stress formation in trees," *Trees*, vol. 24, no. 1, pp. 105–115, 2010.

[81] N. P. van Dijk, E. K. Gamstedt, and I. Bjurhager, "Monitoring archaeological wooden structures: Non-contact measurement systems and interpretation as average strain fields," *Journal of Cultural Heritage*, vol. 17, pp. 102–113, 2016.

Acta Universitatis Upsaliensis

Digital Comprehensive Summaries of Uppsala Dissertations from the Faculty of Science and Technology 2322

Editor: The Dean of the Faculty of Science and Technology

A doctoral dissertation from the Faculty of Science and Technology, Uppsala University, is usually a summary of a number of papers. A few copies of the complete dissertation are kept at major Swedish research libraries, while the summary alone is distributed internationally through the series Digital Comprehensive Summaries of Uppsala Dissertations from the Faculty of Science and Technology. (Prior to January, 2005, the series was published under the title "Comprehensive Summaries of Uppsala Dissertations from the Faculty of Science and Technology".)

Distribution: publications.uu.se
urn:nbn:se:uu:diva-514316

ACTA UNIVERSITATIS
UPSALIENSIS
2023